SAO-AXAF-DR-94-082
Data Type: 3
Rev "A"
March 1994

Advanced X-Ray Astrophysics Facility (AXAF)

Mission Support

NAS8-36123

Performance Reports:

Mirror Alignment System Performance Prediction Comparison Between SAO and EKC

Prepared in accordance with DRD# 784MA-002

Principal Investigator

Dr. H. D. Tananbaum

Prepared for:
George C. Marshall Space Flight Center
National Aeronautics and Space Administration
Marshall Space Flight Center, AL 35812

Submitted by:
Smithsonian Astrophysical Observatory
60 Garden Street
Cambridge, MA 02138

SAO-AXAF-DR-94-082
Data Type: 3
Rev "A"
March 1994

Advanced X-Ray Astrophysics Facility (AXAF)

Mission Support

NAS8-36123

Performance Reports:

Mirror Alignment System Performance Prediction Comparison Between SAO and EKC

Prepared in accordance with DRD# 784MA-002

Principal Investigator

Dr. H. D. Tananbaum

Prepared for:
George C. Marshall Space Flight Center
National Aeronautics and Space Administration
Marshall Space Flight Center, AL 35812

Submitted by:
Smithsonian Astrophysical Observatory
60 Garden Street
Cambridge, MA 02138

The Smithsonian Astrophysical Observatory
is a member of the
Harvard-Smithsonian Center for Astrophysics

Smithsonian Institution
Astrophysical Observatory

Title: Performance Reports:
Mirror Alignment System Performance
Prediction Comparison-Between
SAO and EKC

Date: 14 Mar 1994

Document No.: SAO-AXAF-DR-94-082

DRD No.: 784MA-002

Prepared by: J.P. Zhang

Data Type: 3

Filename: (c:MA002.082)

Revision: "A"

APPROVAL SIGNATURES

F. Cowan330 3/29/94

DEPUTY Program Manager Date

Smithsonian Institution
Astrophysical Observatory

REVISION HISTORY

Title: Performance Reports:
Mirror Alignment System Performance
Prediction Comparison-Between
SAO and EKC

Date: 14 Mar 1994

Document No.: SAO-AXAF-DR-94-082

DRD No.: 784MA-002

Prepared by: J.P. Zhang

Data Type: 3

Filename: (c:MA002.082)

Revision: "A"

Revision Record

Revision	Date	DCO No.	Affected Pages
"A"	14 Mar 1994	-------	Initial Release

Table of Contents

SUMMARY

Distortions of the AXAF High Resolution Mirror Assembly(HRMA) mirrors will be present at zero g during on–orbit operations due to its assembly on the ground in a one g environment. These distortions will be introduced at each stage of assembly as the various parts and subcomponents are added to the HRMA. One of the most important objectives of the HRMA design and assembly effort is to minimize these residual distortions. The AXAF telescope contractor, Eastman Kodak, has identified the HRMA assembly sequence and has provided error budgets for residual distortions introduced in each assembly step. The SAO mission support team has continually reviewed Kodak's work in this area and is performing parallel analyses of several of the larger assembly error budget terms

The largest predicted residual distortion attributed to the assembly process occurs when the mirrors are bonded to the mirror support pads after the mirror has been aligned within the HRMA. During alignment and bonding the mirrors are supported by the Kodak Mirror Alignment System (MAS), one of the most important pieces of ground support equipment which will be used by Kodak during assembly and alignment of the HRMA. The functions of the MAS are to support the miror in as near to a strain–free state as possible during alignment and bonding and provide the articulation of the mirror necessary for alignment of the mirror within the HRMA

Residual mirror distortions resulting from the assembly process may be divided into two categories: 1) **nominal** distortions, which are those inherant to the design and usage of the equipment, even if the mirror support is ideal, and 2) **variational** distortions, which arise due to non–ideal support of the mirrors by the MAS.

We have analyzed both types of distortions described above. The **nominal** distortions were computed using a deterministic finite element analysis, assuming perfect support of the mirror by the MAS. These distortions are very small, their overall performance impact on the HRMA being less than 0.01 arcsec(90% encircled energy diameter). The **variationa**l distortions were computed using an SAO developed Monte–Carlo statistical technique, since the MAS support errors are statistical in nature, and compared to Kodak's results.

The SAO MAS performance predictions in terms of the 90% encircled energy(EE) diameters are shown in the table on the following page, along with predictions by Kodak. SAO, using a Gaussian distribution for MAS errors and for a total of 1000 sample cases, predicts an overall HRMA variational strain due to the MAS of 0.1626 arcsecond as compared to the Kodak prediction, using a 'truncated Gaussian' distribution and a total of 50 sample cases, of 0.1911 arcsecond. If, however, a uniform distribution is used then SAO's prediction is 0.2394 arcsecond, somewhat larger than the Kodak prediction.

The differences between the SAO and Kodak predictions are due mainly to the following sources:

1. In the MAS force sensitivity analysis, (a) the different finite element mirror models are used by Kodak and SAO, and (b) an inaccurate result obtained by Kodak (when a unit radial moment was applied to the optic).
2. Different random error distributions used by Kodak and SAO in the Monte–Carlo analysis. Kodak used a truncated Gaussian while SAO used both a true Gaussian and a uniform distribution.
3. Different numbers of cases run, hence different error statistics.

	P1/H1	P3/H3	P4/H4	P6/H6	HRMA
EKC(trunc Gauss)	0.20360	0.15720	0.16890	0.04264	0.19110
SAO(Gaussian)	0.16400	0.11708	0.13049	0.04171	0.16262
SAO(uniform)	0.28767	0.29286	0.26588	0.07133	0.23944

Units in arcseconds

Monte–Carlo 90% Encircled Energy Performance Comparison, SAO/Kodak

All of the above predictions fall within the Kodak CDA error budget for this error term, which is 0.26 arcseconds. However, these predictions are based on design data for the MAS, not on measured data. For both verification and performance prediction purposes, therefore, we must have measured data for the MAS error magnitudes and their statistics. This data must be measured as part of the verification program for the MAS. This is especiallly critical due to the sensitivity of HRMA performance to MAS errors.

Mirror Alignment System
Performance Prediction Comparison – Between SAO and EKC

March 14, 1994

J. P. Zhang

1.0 INTRODUCTION

Distortions of the AXAF High Resolution Mirror Assembly(HRMA) mirrors will be present during on–orbit operations, at zero g, due to its assembly on the ground in a one g environment. These distortions will be introduced at each stage of assembly as the various parts and subcomponents are added to the HRMA. One of the most important objectives of the HRMA design and assembly effort is to minimize these residual distortions. Early AXAF studies indicated that a vertical assembly process, in which the HRMA is assembled with its optical axis vertical(aligned with gravity) would produce significantly less residual assembly distortion than would a horizontal assembly process, as had been used in prior X–ray programs. The AXAF program and telescope contractor, Eastman Kodak, have therefore planned for vertical assembly of the HRMA. Kodak has determined the HRMA vertical assembly sequence and is developing the necessary facilities and ground support equipment to perform this task. They have also developed error budgets for the residual distortions for each assembly step and have performed analyses of the process and equipment to demonstrate that the AXAF performance requirements are met using their process.

The SAO mission support team has been reviewing Kodak's work in this area since the initiation of the program and is now performing analyses of several of the larger assembly error sources. The largest currently predicted residual distortion attributed to the assembly process occurs when the mirrors are bonded to the mirror support pads after the mirror has been aligned within the HRMA. During alignment and bonding the mirrors are supported by the Kodak Mirror Alignment System (MAS), one of the most important pieces of ground support equipment which will be used by Kodak during assembly and alignment of the HRMA. A pictorial of the MAS is shown in Figure 1.

During assembly each optic is supported on one of its' ends(wide end from below for the paraboloids and narrow end from above for the hyperboloids) by three equally spaced(120 degrees apart) hard points, which determine the optics' rigid body orientation. To minimize mirror distortions due to gravity during assembly, nine additional vertical forces are applied to the ends of the optic, three forces between each two hard points, nominally spaced 30 degrees apart. These forces are provided by offloader mechanisms and are called offload forces. A perfect optic support would, therefore, consist of 12 equal forces, each being 1/12 of the optic weight, spaced precisely 30 degrees apart. The radial positions of the forces would also be equal, chosen so as to minimize optic distortion. However, even if the optic support is perfect as designed, it is still distorted due to the location on the end and the point load nature of the supporting forces. The distortions from a perfectly supported(by the MAS) optic have been called(by Kodak) nominal HRMA assembly strains and may be calculated using a deterministic finite element analysis followed by a raytrace.

Additional distortions are produced due to the non–ideal nature of the supports. Tolerances in the MAS support system will introduce variations in the vertical forces, small radial or tangential forces or variations in the positions at which the forces are applied. The errors introduced by the MAS tolerances can be converted into forces and moments at 12 supporting locations on the MAS: the 3 hard

points and the 9 offloaders. Since the force and moment errors at each of the 12 supports of each mirror are independent(from each other) and random and the total residual distortion in any single mirror is a function of these independent, random error sources, then the combination of errors for a mirror pair is also random. A Monte–Carlo technique is applied to calculate the residual distortions for each mirror pair. The statistical result obtained from the Monte–Carlo analysis provides the mirror performance prediction for these random errors. This error term has been called an unknown bias variation in Kodak's error budget, since it is fixed at assembly time but unknown in magnitude.

The objective of this study is to perform an independent analysis of the residual HRMA mirror distortions caused by force and moment errors in the MAS to statistically predict the HRMA performance. These performance predictions are then compared with those performed by Kodak as a verification of their analysis work.

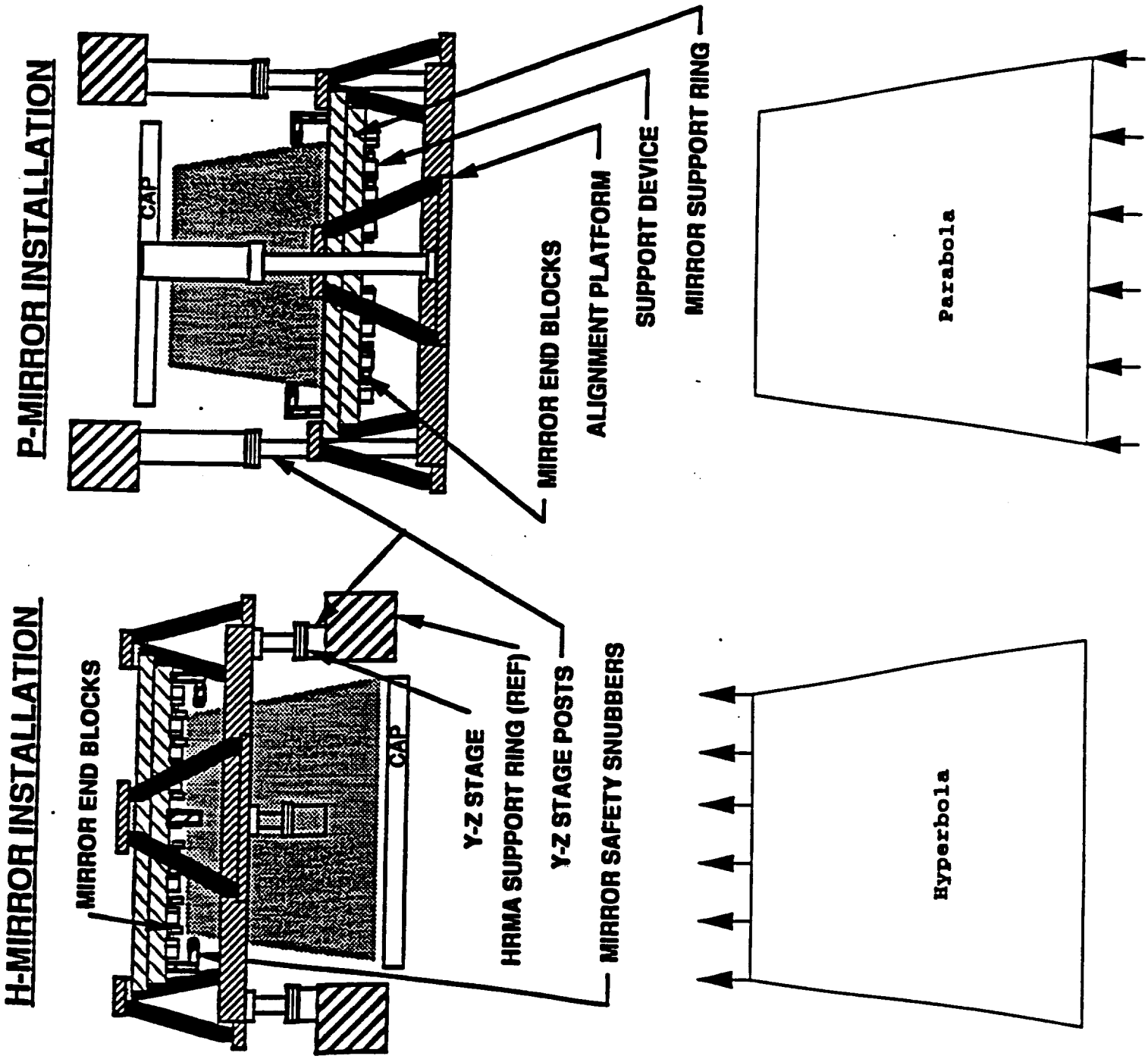

Figure 1 – Mirror Assembly System Schematic

2.0 OVERVIEW of METHODOLOGY

2.1 Nominal Assembly Strain

An analysis of nominal HRMA assembly strain was performed on the P3/H3 mirror pair. To simulate the release of 1g gravity when in orbit, a superposition analysis method was applied in the finite element analyis. In this analysis, the mirrors were assumed to be supported by the MAS perfectly. In the first the mirror alone was supported at 12 equally spaced supporting points: 3 hard points and 9 offloaders. An axial load (–Z direction) of 1/12 of the mirror's weight was applied at each offloader. The axial and theta directions were restrained at each hard point. A 1g gravity in the +Z direction was applied to the mirror. In the second case the mirror was connected to the Mirror Support Sleeves (MSS). The sleeve was fixed to the CAP. The 1g gravity was reversed in the –Z direction, and an axial load (+Z direction) of 1/12 of the mirror's weight was applied at each of the 12 supporting points. Also the same amount of reaction forces (theta) obtained from mirror only case was applied at the hard points but in the opposite direction. Superimposing the above two cases will give the desired nominal residual strain. The P3 and H3 mirror displacements were fit by Legendre–Fourier polynomials. The ray trace of the P3/H3 mirror pair shows a very small 90% EE diameter of 0.0063 arcsec.(Kodak's results show zero values for two decimal places).

2.2 MAS Variational Assembly Strain

The MAS variation analysis is performed in two steps: 1) the MAS force sensitivity analysis and 2) the Monte–Carlo analysis. In the MAS force sensitivity analysis, an error (a unit load , force or moment depending on the degree of freedom (DOF) in finite element analysis) is applied to either a hard point or offloader in the finite element model as an independent analysis case. The residual distortions caused by the error are then fit by Legendre–Fourier polynomials. For each mirror the combination of all Legendre–Fourier coefficient sets (corresponding to all independently analyzed cases) forms a MAS force sensitivity matrix. The MAS force sensitivity matrix contains all the mirror deformations (residual distortions) due to unit loads applied at each DOF of the 12 support locations. In the Monte–Carlo analysis a set of independent random errors (corresponding to tolerances at all 6 degrees of freedoms) are generated for each DOF at each of the 12 locations per each mirror. These random errors are used as multipliers to scale the MAS sensitivity matrix. The scaled matrix is then superimposed into a set of Legendre–Fourier coefficients which contains the random combination of overall residual distortions in the mirror caused by all possible errors. The resulting performance prediction is only one statistical case, based on the randomly selected errors. The above processes must be repeated many(N) times to obtain a reliable statistical result. Raytracing of the Legendre–Fourier coefficient sets for each P–/H– mirror pair gives N values of the RMS and 90% Encircled Energy (EE) diameters. The sorted results of these N values predict statistically the MAS performance for the mirror pair.

3.0 DETAILED DISCUSSION and RESULTS

3.1 MAS Force Sensitivity Analysis

An MAS force sensitivity analysis was conducted for all P– and H–mirrors in order to obtain information on the variability effects of the assembly process. The result of the MAS force sensitivity analysis was used to generate a sensitivity matrix for each of the P– and H–mirrors. The MAS sensitivity matrix containing all the mirror deformations was then used in the Monte–Carlo analysis.

In the mirror assembly process all of the possible errors are converted into forces and moments at the 3 hard points and the 9 offloaders. In the MAS sensitivity analysis a unit load (force or moment) was applied to the finite element mirror model at each of 6 degrees of freedoms (non–restrained DOF only). Thus in the finite element analysis (FEA), the possible errors are associated with each non–restrained degree of freedom at each location (hard point or offloader).

3.1.1 Finite Element Analysis

In the MAS assembly process, the mirror was first supported at three hard points in the tangential and axial directions. The possible errors (forces or moments) exist at hard points and offloaders for all degrees of freedom that are not restrained. For this case no gravity is considered due to the fact that in the variation analysis we are only concerned with the 'variation from nominal'. The mirror is then connected and bonded to the Mirror Support Sleeves (MSS) which are supported by Central Aperture Plate (CAP). The supports at the hard points and offloaders are removed from the mirror. The residual strain in the mirror following this process provides the variational residual distortions in the MAS.

To simulate the MAS assembly process and obtain the MAS force sensitivity corresponding to the applied loads, a superposition analysis method was applied in the finite element analysis. Unit loads (forces or moments) were applied instead of the 'actual' loads. Figure 2 shows 12 locations of the hard points and offloaders. A 360 degree SDRC–IDEAS FEA model for the P1 mirror and MSS is shown in figure 3 (Note: All models were originally generated using ANSYS and we then later "read–in" and re–created by IDEAS. The IDEAS models were rechecked against the original ANSYS models.). The mirror is modeled by solid elements. In the analysis, a unit load (force or moment) was applied at each of 12 points for all unrestrained degrees of freedom, one load at a time. By applying the superposition method , we first analyzed the mirror only, that is, the mirror is disconnected from the MSS. A unit load was applied at the hard point or offloader in each independent analysis. The mirror was supported (restrained) at three hard points in the tangential (θ) and axial (Z) directions. We then analyzed the case when the mirror is connected to and supported by the MSS and the MSS is fixed to the Central Aperture Plate (CAP). The same unit load is now applied at the same

hard point or offloader but in the opposite direction. Also the same amount of reaction forces obtained from the mirror only case were applied at the hard points but in the opposite direction. Superposition of these analyses will give the desired residual strain in the mirror which reflects the force sensitivity of the mirror corresponding to the applied load. To complete the full MAS sensitivity study, independent analysis at two offloaders B10 and C7 (ref. figure 2) and one hard point A1 were needed to provide all possible force and moment sensitivity cases. In practice, by making full use of the symmetry in geometry and loading, we did not have to perform analysis and data fitting for all hard points and offloaders. The results for other hard points and offloaders can be derived from A1, B10 and C7(see below for details).

The mirror displacements subjected to a unit load obtained from FEA are fit by Legendre–Fourier polynomials. The SAO TransFit software package was used to perform the superposition and to calculate the Legendre–Fourier coefficients. The low order deformations caused by the MAS residual errors are well–fit by Legendre–Fourier polynomials.

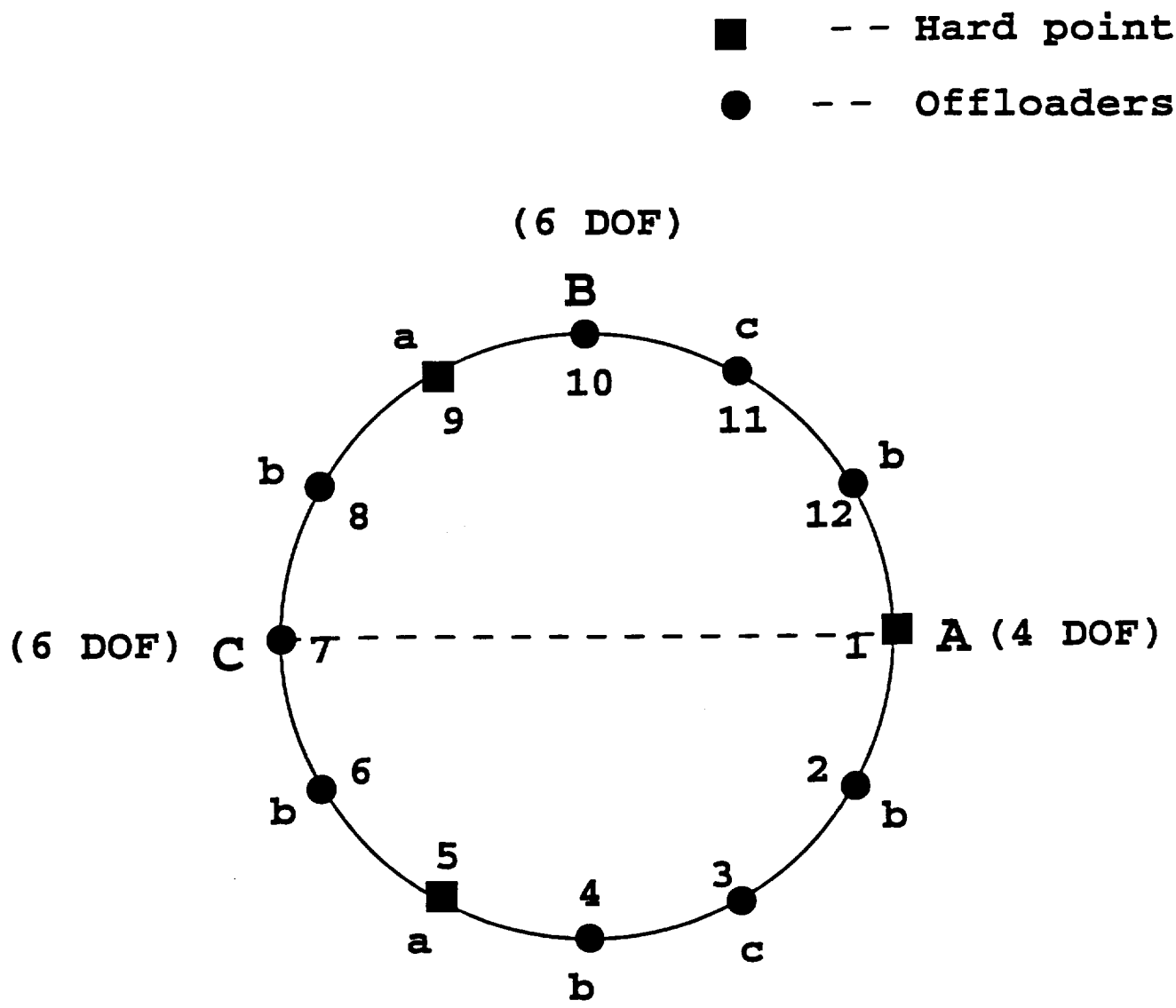

Figure 2 – 12 Mirror Support Locations

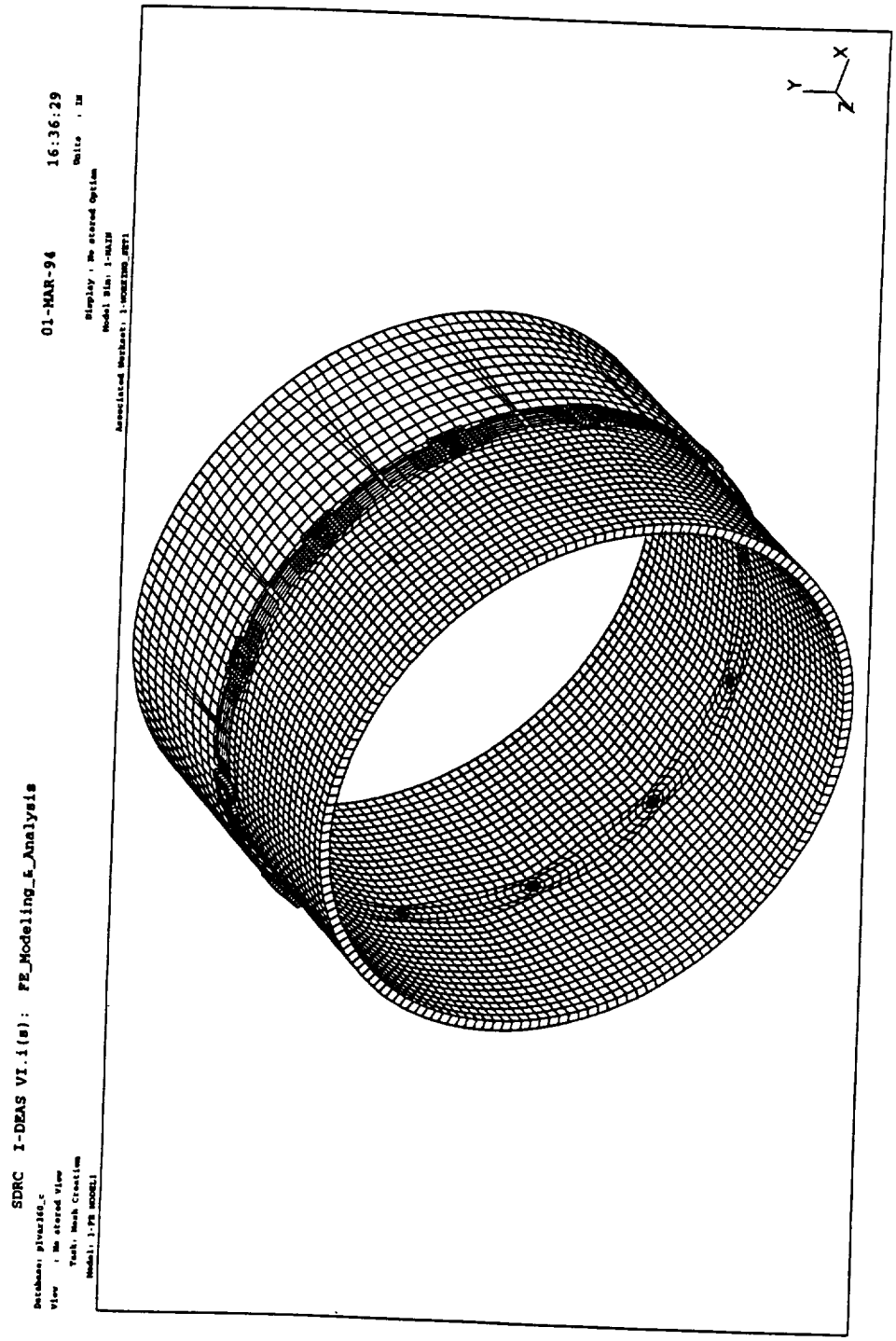

Figure 3 – Mirror Finite Element Model

3.1.2 Force Sensitivity Result Comparison

Among the Legendre–Fourier coefficients, six coefficients which represent decenter, tilt, ovalization, delta–delta r ($\delta\delta$ r), trefoil, and delta trefoil (δ trefoil) are listed in Appendix A and compared with those analyzed by EKC. Our results show that for all P– and H– mirrors, the Legendre–Fourier coefficients agree with EKC within a reasonable range(the discrepancy is due mainly to the different finite element models used by EKC and SAO) except in DOF 4 (a moment applied in the radial direction) where a large error (up to several hundred percent difference in $\delta\delta$ r) is found. A further raytrace study on Legendre–Fourier coefficient sensitivity shows that errors in most coefficients are negligible since the terms themselves have a very small impact on system performance. However, the disagreement in $\delta\delta$ r for DOF 4 can have a noticeable impact on the MAS performance prediction. In order to determine the impact on the MAS performance prediction due to the discrepancy of the MAS force sensitivity analysis between EKC and SAO, we raytraced 6 Legendre–Fourier coefficients (decenter, tilt, ovalization, $\delta\delta$ r, trefoil and δ trefoil) for the P1 and P6 mirrors (ref. [1], attached in appendix B). In each independent raytrace, one out of the six Legendre–Fourier coefficients was singled out by setting others to zero(A value of 10 μin was applied to each coefficient except the tilt where a value of 0.1 arcsecond was used). The raytrace results were then scaled to obtain the 90% EE diameter for all DOFs at hard point A and offloaders B and C. Table 1 in [1] shows that the large discrepancy in the Legendre–Fourier coefficients for DOF 4 has a negligible impact on the 90% EE diameter for all terms except $\delta\delta$r, where the difference in the 90% EE between EKC and SAO is approximately 0.06 arcsecond for P1 and 0.027 arcsecond for P6 with a unit(1 in–lb) applied load. Since the DOF 4 tolerances are 0.684 in–lb for the P1 mirror and 0.2445 in–lb for the P6 mirror, the $\delta\delta$ r discrepancy at DOF 4 alone could have an impact on 90% EE of 0.041 and 0.007 arcsecond for the P1 and P6 mirrors, respectively. An effort to determine the cause of the discrepancy in DOF 4 was made by analyzing different shell and solid element FEA models (since EKC used shell elements and SAO used solid elements to model the P– and H–mirrors). A consistent result is observed for the solid element models when changing the mirror element's circumferential size, however, the result from the shell elements models is mesh dependent due to the fact that a shell element cannot sustain a moment perpendicular to its plane. In fact, continuing reduce the mesh's circumferential size will result in a larger deformation or even a singularity as the angle between a bending moment (in DOF 4) and the normal of the shell element plane tends to 90 degree (ref. [1]).

3.2 Monte–Carlo Analysis

A Monte–Carlo technique is used to randomize the variation for each possible error in the analysis. The technique is utilized to predict statistically the impact of the variations on the mirror pairs and the HRMA system performance.

In the Monte–Carlo analysis a set of independent random errors are generated at each location and for each degree of freedom. The tolerances (allowable maximum errors) at each DOF for all mirrors are listed below in Table 1 (ref. [2]). Random errors based on these tolerances are then used as multipliers to scale the MAS sensitivity matrix obtained from the MAS force sensitivity analysis. The resulting summation of the coefficients of all the errors then forms a single Legendre–Fourier coefficient set for each mirror. The two (P–/H–) mirrors may then be raytraced to determine the system performance **given that particular set of random MAS errors**. The above process may be repeated (independent random errors are generated for each run) as many times as desired to obtain statistically the Monte–Carlo MAS performance prediction (in terms of the RMS and 90% EE diameter).

	Force (lb)			Moment (in–lb)		
Optic	**DOF 1**	**DOF 2**	**DOF 3**	**DOF 4**	**DOF 5**	**DOF 6**
P1	0.0522	0.0382	0.0500	0.6840	0.1270	0.0110
P3	0.0326	0.0238	0.0500	0.4265	0.0792	0.0110
P4	0.0260	0.0190	0.0500	0.3402	0.0632	0.0110
P6	0.0187	0.0137	0.0500	0.2445	0.0454	0.0110
H1	0.0499	0.0365	0.0500	0.6535	0.1213	0.0110
H3	0.0311	0.0228	0.0500	0.4078	0.0757	0.0110
H4	0.0248	0.0182	0.0500	0.3278	0.0604	0.0110
H6	0.0178	0.0131	0.0500	0.2337	0.0434	0.0110

Table 1 – MAS Tolerances

The Monte–Carlo analysis flow chart (for one optic) is shown in Figure 4. A detailed discussion for each step is listed on the following pages.

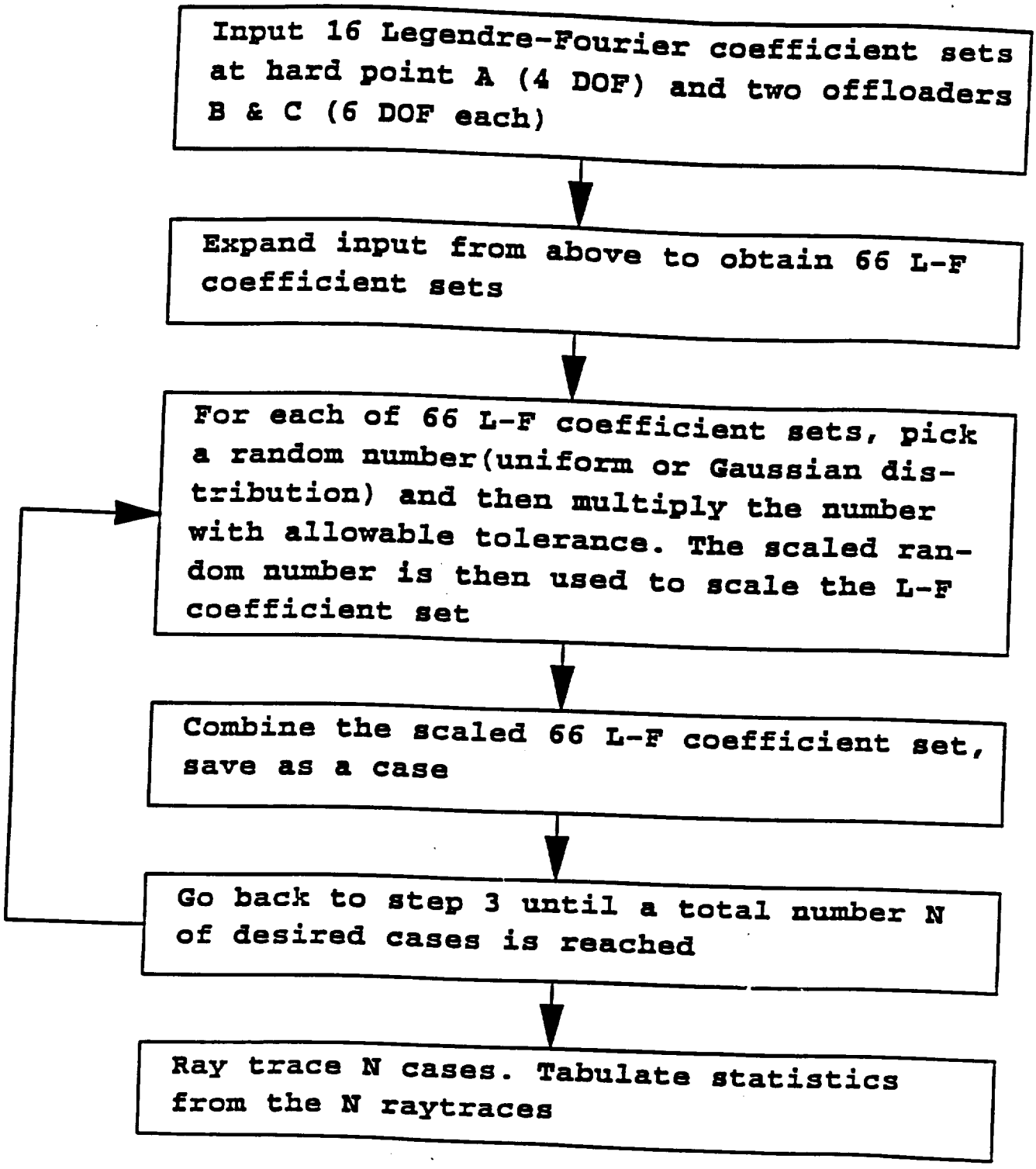

Figure 4 – Monte–Carlo Analysis Flow Chart

(1) Input 16 Legendre–Fourier coefficient sets

Figure 2 shows 12 mirror supports: 3 hard points (each hard point has 4 possible errors associated with 4 non–restrained DOF) and 9 offloaders (each offloader has 6 possible errors associated with 6 non–restrained DOF), a total of 66 possible errors associated with 66 non–restrained DOF. In the MAS force sensitivity analysis, the mirror deformation corresponding to each unit load is fit with Legendre–Fourier coefficients (SAO uses 10 Legendre terms and 13 Fourier terms which is the same as used by EKC. Each coefficients set at SAO contains 270 coefficients: 10 Legendre coefficients represent azimuthally invariant deformation, 260 Fourier coefficients (130 each in cosine and sine) represent azimuthally variant deformations). Therefore, the MAS sensitivity matrix containing mirror deformation due to the 66 unit loadings would have a size of 66 by 270. In practice, by making use of the symmetry in geometry and loading, we do not have to perform analysis and data fitting for all 66 unit loadings to obtain the 66 Legendre–Fourier coefficient sets. In fact only 16 Legendre–Fourier coefficient sets (4 sets at hard point A1 and 6 sets each at offloaders B10 and C7) are need (refer to Figure 2). We developed a FORTRAN program to derive the other sets via mirroring and phase angle rotation of Fourier coefficient terms (refer (2) below for details).

(2) Expand input from (1) to form a MAS force sensitivity matrix

Due to the symmetry of the geometry and loading in the problem, the full MAS force sensitivity matrix can be filled by +/– 120^0 phase angle rotations and mirroring across symmetry line from the known coefficient sets in (1). Refer to figure 2, The Legendre–Fourier coefficient sets at hard point a5 and a9 were obtained by a –/+ 120^0 phase angle rotation (Fourier terms only) from hard point A1, respectively. Likewise, a +/– 120^0 phase angle rotation from offloader C7 provided coefficient sets at offloader c3 and c11; and offloaders b3 and b6 were derived from offloader B10 by a –/+ 120^0 phase angle rotation. Coefficient sets at offloader b8 was then obtained from offloader b6 by a reflection (mirroring) across the symmetry line. The last two offloaders b4 and b12 were obtained by a +/– 120^0 phase angle rotation from offloader b8. (verification of the results of the Legendre–Fourier coefficients transfer has been made and documented in [3]).

(3) Apply scaled random numbers to scale MAS force sensitivity matrix

A total of 66 random numbers are generated using a random number distribution (Gaussian distribution, uniform distribution, etc.). In a uniform distribution, random numbers are generated in the range of [–1, 1] "uniformly", while in a Gaussian distribution, a mean value of zero and a standard deviation of 1/3 (assumes that the tolerances are of 3σ values) are chosen to determine the Gaussian distribution function so that the random numbers generated are not limited to the range of [–1, 1]. The random numbers were then scaled by the allowable tolerances (listed in Table 1) according to their DOF, and finally the scaled 66 random numbers were used to scale the MAS force sensitivity

matrix.

(4) Combine the scaled matrix to a Legendre–Fourier coefficient set

Combine (superimpose) the matrix elements of the same Legendre–Fourier coefficient terms into one Legendre–Fourier coefficient set which contains all error contributors from each degree of freedom at all 12 supports. This set is ready to perform a single ray trace as a sample case.

(5) Repeat steps (3) to (4) until a number N (total desired sample cases) is reached

A proper number N is required to ensure a reliable statistical result. Note that in each run from (3) to (4), a different seed number was used (in a subroutine where a series of random numbers are generated) to ensure an independent series of random numbers been chosen.

(6) Ray trace N cases

For each of the N sample cases saved in step (4), ray trace Legendre–Fourier coefficient set for each P–/H–mirror pair to obtain the RMS and 90% EE diameters. The MAS performance prediction for the mirror pair is obtained from the statistics of the N cases.

The ensemble HRMA performance prediction(all four mirror pairs) can be obtained by combining mirror pair results according to the effective area of each mirror pair. The effective areas (at 0.107 Kev) for the four mirror pairs and the percentage of the total area for each mirror pair are listed in Table 2. The percentage of the each mirror pair is scaled to the total number of rays to determine the number of rays to be traced in each mirror pair. For each of the N sample cases the summation of the 4 pairs gives the results in terms of the RMS and 90% EE diameters for that case. The HRMA Monte–Carlo performance prediction (the 3σ confident level) is based on the statistics of the N sample cases.

Mirror Pair	Effective Area* (cm^2)	Percentage %	Number of rays
P1/H1	415.921	39.80	3980
P3/H3	276.262	26.44	2644
P4/H4	227.151	21.74	2174
P6/H6	125.656	10.02	1202
Total	1044.990	100.00	10000

* The effective areas are calculated at 0.107 Kev

Table 2 – Effective Areas for Each Mirror Pair

In the Monte–Carlo analysis, the type of random number distribution used in the analysis is important since using a different random number distribution leads to a different MAS performance prediction. For instance, assuming that the tolerances for all degrees of freedoms listed in Table 1 are 3σ values, that is the errors (forces or moments) fall into a Gaussian distribution pattern, then a Gaussian distribution should be used to generate the random numbers in the Monte–Carlo analysis. Assuming however that the errors at a specific DOF do not exceed an allowable tolerance and the errors fall into a flat pattern, then a uniform distribution should be used for that DOF. The actual error distribution pattern can be determined based on a set of tests on the mirror assembly station hardware(not available at present).

3.3 Result Comparison

A Gaussian distribution was used at SAO under the assumption that the tolerances are 3σ values. This means that there is a 68.3% chance that the actual errors are within 1σ range (1/3 of the tolerances), a 99.74% chance that the actual errors are within 3σ range. To determine qualitatively the impact on the Monte–Carlo analysis result due to different random number distributions, a uniform distribution (the random numbers are generated within the tolerances 'uniformly') was also analyzed at SAO. Table 3 lists the 90% EE diameters comparison of a Gaussian distribution against a uniform distribution for 10 separate trials of the P1/H1 mirror pair. The RMS or 90% EE diameter obtained by a uniform distribution for all possible errors is about 42% in average greater than that obtained by a Gaussian distribution. Since a uniform distribution always predicts a larger value of the RMS and 90% EE diameters than a Gaussian distribution, it is important to use the proper distribution in the Monte–Carlo analysis to obtain an accurate MAS performance prediction. Ideally, a set of tests on the mirror assembly station hardware should be performed. If the measured errors at a specific DOF do not exceed an allowable tolerance and the errors show a flat distribution pattern, then a uniform distribution should be used for that DOF. On the other hand, if the test results show a normal distribution pattern at a specific DOF, then a Gaussian distribution should be used to that DOF.

	1	2	3	4	5	6	7	8	9	10	Err %
Gaussian	0.1244	0.1441	0.1230	0.1518	0.1295	0.1752	0.1661	0.1372	0.1640	0.1413	30
Uniform	0.2455	0.2869	0.2391	0.2790	0.2484	0.2118	0.2539	0.2333	0.2877	0.2367	26
%	49	50	49	46	48	17	35	41	43	40	

Unit in arcsec. *The listed result of each test case is the 100th data from its sorted data set.

Table 3 – P1/H1 pair 90% EE diameters of 10 independent Monte–Carlo analysis using a Gaussian and a uniform distribution (N=100)*

A 'truncated Gaussian' distribution was used at EKC in their Monte–Carlo analysis. A 'truncated Gaussian' distribution uses a Gaussian distribution function to generate random numbers but it truncats (filters out) random numbers that are larger than the tolerances. The reason for using a 'truncated Gaussian' distribution, according to EKC, is that during the mirror alignment process, EKC will realign the mirror if any measured error exceeded the allowable tolerance. One concern to the 'truncated Gaussian' distribution is that since the distribution is mathematically not a Gaussian distribution, the MAS performance prediction (3σ confidence level) should be the largest data in the sorted data set (not the 997^{th} data as in a Gaussian distribution when N=1000). This is due to the fact that 0.3% (the extension of the 3σ value) has been truncated from the Gaussian distribution, and all errors are forced to be within the allowable tolerances. Conseqently, the largest value in the set of N cases (as in a uniform distribution) should be used to give the performance prediction.

The Monte–Carlo MAS performance predictions are based on the statistics of the analyzed sample cases. A proper number of the samples(N) is required to ensure a reliable result. EKC used 50 sample cases (N=50) in their analysis. Our results show that N=50 is not sufficient. Table 3, above, shows results for 10 independent Monte–Carlo analyses (N=100) using a Gaussian distribution for the P1/H1 mirror pair. In each independent anaysis, the 100^{th} data in the sorted data set was chosen as the 3σ confident level. A maximum error of 30% is observed. A further Monte–Carlo analysis was performed at SAO in an attempt to determine a proper number of trials, N, to be used in the analysis. We chose test cases of N=25, 50, 100, 150, 200, 250, 500 and 1000. Corresponding to each N a set of independent analysis was performed to obtain the 90% EE diameter in terms of the mean value and the standard deviation, as shown in Table 4. Figure 5 shows three curves of the 90% EE diameter(mean value, mean value+σ, and mean value–σ) against the trail number N. A convergent pattern is observed as N increases. The results indicate that as the number of samples, N, increases, the 90% EE mean value increases and it tends to 0.1680 arcsecond when N=1000. Also the standard deviation drops from 0.019 at N=50 to 0.009 at N=500. The analysis results clearly indicate that N=50 is not sufficient, instead a value of $N \geqq 500$ is suggested to obtain a more accurate performance prediction. The test results shown by EKC (ref. [4]) for N=25, 50, 75 and 100 were based on (1) one run of the Monte–Carlo analysis for N=100, and (2) an analysis of dependent raw data sets (for instance, the

raw data set of N=50 includes raw data set of N=25; the raw data set of N=100 includes data sets of N=25, N=50 and N=75), which we believe is not appropriate. In fact it is quite possible that the maximum data in the 100 data set is located among the first 25 data (because of the randomization in the analysis). If that is the case then by following EKC analysis, N=25 would be sufficient since the same result can be obtained for $N \geqq 25$.

	Mean Value	Standard Deviation	Max Err. %**
N=25	0.13244	0.02070	66
N=50	0.14768	0.01900	60
N=100	0.15805	0.01771	45
N=150	0.15520	0.01154	27
N=200	0.15670	0.01046	23
N=250	0.15801	0.01118	23
N=500	0.16339	0.00897	15
N=1000	0.16800	0.00607	7

Unit in arcsecond ** Max Err. % = [(Max value – Min value) /(Mean value)]x100%

Table 4 – P1/H1 mirror pair statistics 90% EE diameter for various sample cases

Table 5 shows the Monte–Carlo performance predictions (in terms of RMS and 90% EE diameters) for the HRMA and for each of the mirror pairs using a Gaussian, a uniform and a 'truncated Gaussian' distribution. Table 5 also lists results analyzed at SAO using a 'truncated Gaussian' distribution for N=50, this is intended for a proper comparison with EKC (since a 'truncated Gaussian' distribution and N=50 were used at EKC). The results at SAO for a Gaussian distribution are based on N=1000 sample cases. The listed RMS and 90% EE diameters are the 997^{th} data (3σ confident level) chosen from the sorted data set. As a reference the results using a 'truncated Gaussian' distribution for N=1000 in the Monte–Carlo analysis are also listed. For a 'truncated Gaussian' distribution (N=50), SAO predicts the 90% EE diameters of 0.126, 0.133, 0.101 and 0.033 arcsecond for the P1/H1 – P6/H6 mirror pairs as compared to EKC values of 0.204, 0.157, 0.169 and 0.043 arcsecond. Based on the argument discussed in this section and the analysis results listed in Table 5, we believe that a Gaussian distribution and a value of N=1000 used in the Monte–Carlo analysis would result in a more accurate prediction. The HRMA performance prediction comparison between SAO and EKC yields a 0.1626 arcsecond by SAO(Gaussian distribution, N=1000) against a 0.1911 arcsecond by EKC ('truncated Gaussian' distribution, N=50). Thus we conclude that our results agree with EKC within a certain range, and EKC predictions appear to be conservative.

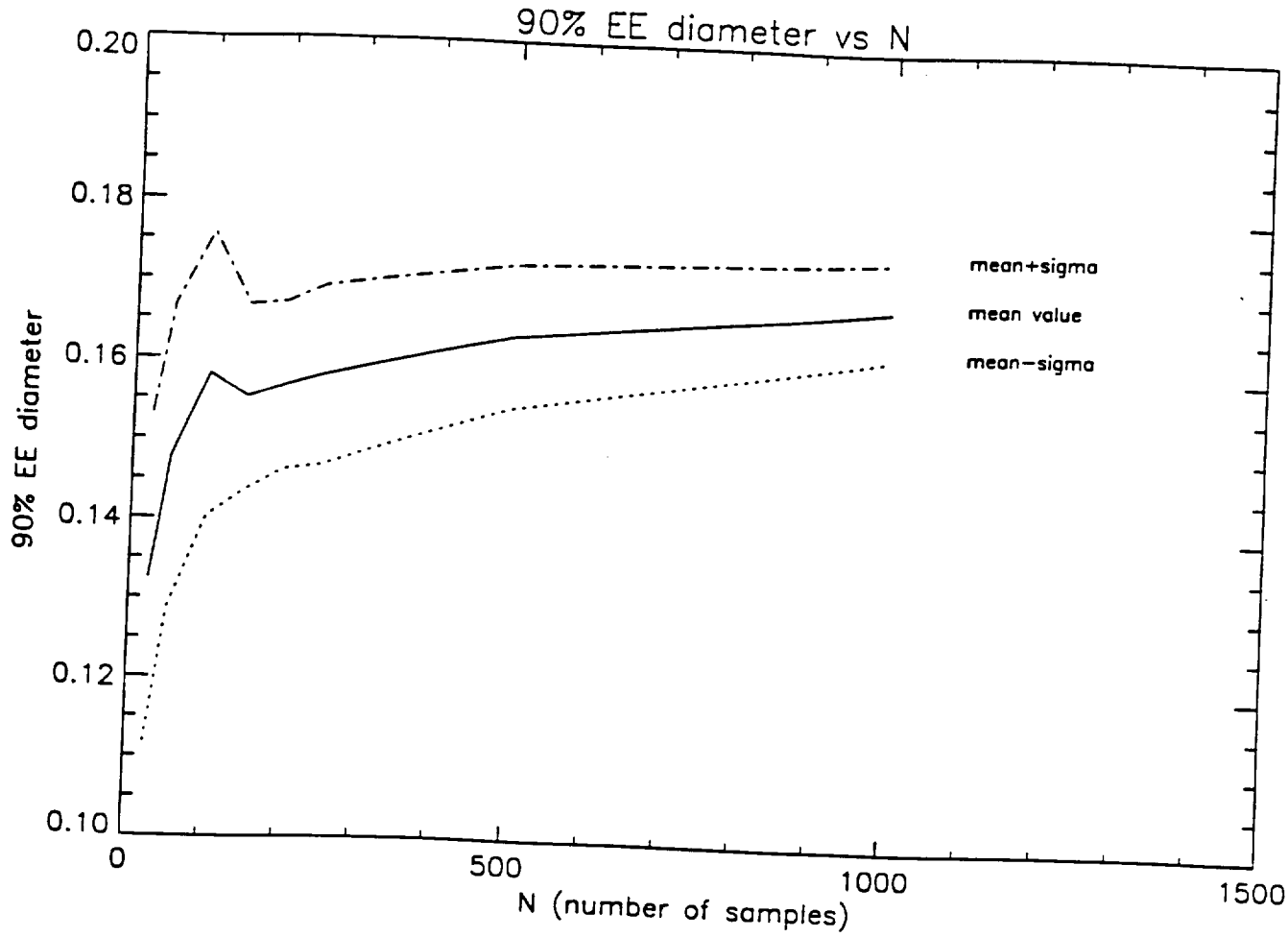

Figure 5 – P1/H1 mirror pair 90% EE diameter vs N

90% Encircled Energy Diameter (3σ confident level)

	P1/H1	P3/H3	P4/H4	P6/H6	HRMA
EKC (N=50) (Truncated Gaussian)	0.20360	0.15720	0.16890	0.04264	0.19110
SAO (N=50) (Gaussian)	0.12438	0.12731	0.12017	0.03416	0.14042
SAO (N=1000) (Gaussian)	0.16400	0.11708	0.13049	0.04171	0.16262
SAO (N=50) (Truncated Gaussian)	0.12591	0.13292	0.10054	0.03321	N/A
SAO* (N=1000) (Truncated Gaussian)	0.16130 0.18606	0.12129 0.15503	0.11638 0.12178	0.03717 0.0502	N/A
SAO(N=1000) (Uniform)	0.2532	0.29286	0.26588	0.07133	0.23944

Unit in arcsec. *Results listed for 'truncated Gaussian distribution' at SAO: the first and second row is the 997th and 1000th data chosen from the sorted data set, respectively.

RMS Diameter (3σ confident level)**

	P1/H1	P3/H3	P4/H4	P6/H6	HRMA
SAO (N=1000) (Gaussian)	0.11419	0.08115	0.08820	0.02838	0.08548
SAO* (N=1000) (Truncated Gaussian)	0.11283 0.12586	0.08436 0.09542	0.07801 0.08540	0.02562 0.03577	N/A
SAO(N=1000) (Uniform)	0.20400	0.20289	0.18800	0.04917	0.13024

Unit in arcsec. **EKC RMS Diameters are not available.

Table 5 – HRMA performance prediction comparison

APPENDIX A

RESIDUAL ERRORS DUE TO UNIT MAS ERRORS

P1 OPTIC

unit in μin

	Hard Point A (DOF 1)			Hard Point A (DOF 4)			Hard Point A (DOF5)			Hard Point A (DOF 6)		
	EKC	SAO	%	EKC	SAO	%	EKC	SAO	%	EKC	SAO	%
Decent	32.80	30.83	6.4	2.525	0.5838	333	0.6487	0.5729	13.2	1.476	1.390	6.2
Tilt	7.111	6.298	12.9	0.6194	0.1621	282	0.2344	0.2062	13.7	0.2632	0.2311	13.9
Oval.	19.25	21.10	8.8	0.1483	0.0308	381	0.0567	0.0614	7.7	0.7848	0.8597	8.7
δδ r	18.70	17.15	9.0	1.770	0.5829	204	0.5692	0.5167	10.2	0.7440	0.6790	9.6
Trefoil	0.2663	0.3348	20.5	0.0099	0.0006	155	0.0027	0.0034	20.6	0.0322	0.0405	20.5
δTrefoil	0.5474	0.5781	5.3	0.1101	0.0129	753	0.0350	0.0363	3.6	0.0653	0.0687	4.9

	Offloader B (DOF 1)			Offloader B (DOF 2)			Offloader B (DOF3)			Offloader B (DOF 4)		
	EKC	SAO	%	EKC	SAO	%	EKC	SAO	%	EKC	SAO	%
Decent	24.71	23.24	6.4	15.53	14.26	8.9	7.304	6.463	13.0	1.622	0.4034	302
Tilt	4.971	4.387	13.3	3.258	3.077	5.9	2.473	2.184	13.3	0.5940	0.1390	327
Oval.	14.37	15.74	8.7	9.024	10.71	15.8	0.2992	0.3246	7.8	0.1399	0.0209	569
δδ r	13.94	12.77	9.1	8.830	8.992	1.8	6.694	6.112	9.5	1.589	0.3926	305
Trefoil	0.2663	0.3352	20.6	0.1235	0.2622	52.9	0.0053	0.0066	19.7	0.0099	0.0006	155
δTrefoil	0.5475	0.5787	5.4	0.2613	0.3418	23.6	0.1427	0.1499	4.8	0.1101	0.0129	753

	Offloader B (DOF 5)			Offloader B (DOF 6)			Offloader C (DOF1)			Offloader C (DOF 2)		
	EKC	SAO	%	EKC	SAO	%	EKC	SAO	%	EKC	SAO	%
Decent	0.8937	0.7917	12.9	1.239	1.159	6.9	9.992	9.299	7.4	22.06	20.78	6.1
Tilt	02747	0.2401	14.4	0.2894	0.2558	13.1	2.377	2.100	13.2	4.528	4.008	13.0
Oval.	0.0659	0.0713	7.6	0.7848	0.8597	8.7	6.491	7.096	8.5	12.76	14.00	8.9
δδ r	0.7857	0.7145	10.0	0.7440	0.6790	9.6	6.215	5.678	9.5	12.49	11.47	8.8
Trefoil	0.0027	0.0034	20.6	0.0288	0.0366	20.7	0.2663	0.3346	20.4	0.1746	0.2201	20.7
δTrefoil	0.0350	0.0363	3.6	0.0583	0.0612	4.8	0.5475	0.5780	5.3	0.3695	0.3921	5.8

	Offloader C (DOF 3)			Offloader C (DOF 4)			Offloader C (DOF5)			Offloader C (DOF 6)		
	EKC	SAO	%	EKC	SAO	%	EKC	SAO	%	EKC	SAO	%
Decent	10.23	9.046	13.1	1.529	0.1797	751	1.020	0.8996	13.4	1.326	1.244	6.6
Tilt	3.515	3.104	13.3	0.4405	0.0524	741	0.3510	0.3081	13.9	0.2508	0.2196	14.2
Oval.	0.4231	0.4591	7.8	0.1311	0.0093	131	0.0739	0.0801	7.7	0.7848	0.8598	8.7
δδ r	9.467	8.644	9.5	1.385	0.1752	691	0.9543	0.8683	9.9	0.7440	0.6792	9.5
Trefoil	0.0075	0.0094	20.2	0.0099	0.0006	155	0.0027	0.0034	21.3	0.0251	0.0316	20.6
δTrefoil	0.2018	0.2121	4.9	0.1101	0.0129	753	0.0350	0.0363	3.6	0.0503	0.0528	4.7

P3 OPTIC

unit in μin

	Hard Point A (DOF 1)			Hard Point A (DOF 4)			Hard Point A (DOF5)			Hard Point A (DOF 6)		
	EKC	SAO	%	EKC	SAO	%	EKC	SAO	%	EKC	SAO	%
Decent	43.16	39.10	10.4	4.005	0.8091	395	0.9654	0.8407	14.8	2.429	2.223	9.3
Tilt	10.23	8.718	17.3	0.9616	0.2615	268	0.3574	0.3037	17.7	0.4759	0.4069	17.0
Oval.	20.04	21.58	7.1	0.1705	0.0129	1222	0.0649	0.0731	11.2	1.016	1.104	7.9
δδ r	25.42	24.19	5.1	2.603	0.7406	251	0.7981	0.7574	5.4	1.271	1.212	4.9
Trefoil	0.1924	0.2599	26.0	0.0061	0.0002	2950	0.0015	0.0020	25.0	0.0291	0.0397	26.7
δTrefoil	0.5932	0.6837	13.2	0.1351	0.0150	801	0.0400	0.0457	12.5	0.0889	0.1028	13.5

	Offloader B (DOF 1)			Offloader B (DOF 2)			Offloader B (DOF3)			Offloader B (DOF 4)		
	EKC	SAO	%	EKC	SAO	%	EKC	SAO	%	EKC	SAO	%
Decent	32.43	29.44	10.2	20.39	18.53	10.0	8.489	7.205	17.8	2.505	0.5629	345
Tilt	7.132	6.088	17.1	4.671	3.996	16.9	2.918	2.483	17.5	0.9288	0.1966	372
Oval.	14.96	16.10	7.1	9.395	10.13	7.3	0.1892	0.1191	58.9	0.1638	0.0096	1606
δδ r	18.95	18.02	5.1	11.98	11.42	4.9	7.397	6.867	7.7	2.353	0.553	326
Trefoil	0.1924	0.2608	26.2	0.0891	0.1212	26.5	0.0001	0.0021	95.2	0.0061	0.0002	2950
δTrefoil	0.5932	0.6833	13.2	0.2813	0.3261	13.7	0.1261	0.9919	87.3	0.1351	0.0151	795

	Offloader B (DOF 5)			Offloader B (DOF 6)			Offloader C (DOF1)			Offloader C (DOF 2)		
	EKC	SAO	%	EKC	SAO	%	EKC	SAO	%	EKC	SAO	%
Decent	1.305	1.142	14.3	2.040	1.851	10.2	13.17	11.82	11.5	28.95	26.32	10.0
Tilt	0.4026	0.3464	16.2	0.5210	0.4465	16.7	3.412	2.907	17.4	6.491	5.551	16.9
Oval.	0.0720	0.0776	7.2	1.016	1.104	7.9	6.756	7.258	6.9	13.29	14.33	7.3
δδ r	1.095	1.035	5.8	1.271	1.212	4.9	8.473	8.036	5.4	16.95	16.16	4.9
Trefoil	0.0015	0.0021	28.6	0.0261	0.0356	26.7	0.1924	0.2599	26.0	0.1260	0.1714	26.5
δTrefoil	0.0400	0.0456	12.3	0.0794	0.0914	13.1	0.5932	0.6835	13.2	0.3979	0.4615	13.8

	Offloader C (DOF 3)			Offloader C (DOF 4)			Offloader C (DOF5)			Offloader C (DOF 6)		
	EKC	SAO	%	EKC	SAO	%	EKC	SAO	%	EKC	SAO	%
Decent	11.89	10.09	17.8	2.371	0.2463	863	1.486	1.289	15.2	2.170	1.980	9.6
Tilt	4.143	3.525	17.5	0.6803	0.0710	858	0.5170	0.4457	16.0	0.4515	0.3861	16.9
Oval.	0.2676	0.1670	60.2	0.1569	0.0043	3549	0.0784	0.0816	3.9	1.016	1.104	7.9
δδ r	10.46	9.712	7.7	2.074	0.2468	740	1.327	1.253	5.9	1.271	1.212	4.9
Trefoil	0.002	0.0032	93.8	0.0061	0.0002	2950	0.0015	0.0020	25.0	0.0227	0.0310	26.8
δTrefoil	0.1784	0.1976	9.7	0.1351	0.0150	801	0.0400	0.0457	12.4	0.0688	0.0792	15.7

P4 OPTIC

unit in μin

	Hard Point A (DOF 1)			Hard Point A (DOF 4)			Hard Point A (DOF5)			Hard Point A (DOF 6)		
	EKC	SAO	%	EKC	SAO	%	EKC	SAO	%	EKC	SAO	%
Decent	44.33	41.23	7.5	4.545	0.8771	418	1.061	0.9511	11.5	2.836	2.430	16.7
Tilt	10.96	9.838	11.4	1.066	0.3347	219	0.4009	0.3587	11.8	0.5781	0.6854	15.7
Oval.	17.79	20.31	12.4	0.1571	0.1205	30.4	0.0612	0.0811	24.5	1.021	1.598	36.1
$\delta\delta_r$	24.19	24.53	1.4	2.573	1.310	96.4	0.7747	0.7695	6.8	1.375	2.118	35.1
Trefoil	0.1569	0.2298	31.7	0.0036	0.0331	89.1	0.0009	0.0021	57.1	0.0268	0.1917	86.0
δTrefoil	0.4145	0.5292	21.7	0.1006	0.0736	36.7	0.0290	0.0360	19.4	0.0706	0.3726	81.1

	Offloader B (DOF 1)			Offloader B (DOF 2)			Offloader B (DOF3)			Offloader B (DOF 4)		
	EKC	SAO	%	EKC	SAO	%	EKC	SAO	%	EKC	SAO	%
Decent	32.25	30.59	8.7	20.93	19.13	9.4	8.066	7.159	12.7	2.767	0.6178	348
Tilt	7.610	7.162	6.3	4.993	4.847	3.0	2.808	2.595	8.2	1.041	0.2357	342
Oval.	13.27	16.04	17.3	8.336	10.43	20.1	0.1050	0.4478	76.6	0.1529	0.0542	182
$\delta\delta_r$	18.03	19.85	9.1	11.40	13.13	13.2	6.258	6.567	4.7	2.334	0.6188	277
Trefoil	0.1569	0.8657	81.9	0.0726	0.5114	85.8	0.0022	0.0948	97.7	0.0036	0.0127	71.7
δTrefoil	0.4145	1.7110	75.8	0.1963	0.9940	80.3	0.0791	0.1263	37.4	0.1006	0.0264	281

	Offloader B (DOF 5)			Offloader B (DOF 6)			Offloader C (DOF1)			Offloader C (DOF 2)		
	EKC	SAO	%	EKC	SAO	%	EKC	SAO	%	EKC	SAO	%
Decent	1.415	1.275	11.0	2.377	2.194	8.3	13.51	12.43	8.7	29.69	26.96	10.1
Tilt	0.4354	0.3857	12.9	0.6346	0.5608	13.2	3.653	3.273	11.6	6.931	6.862	1.0
Oval.	0.0655	0.0899	27.1	1.021	1.496	31.7	5.996	6.831	12.2	11.79	15.09	21.9
$\delta\delta_r$	1.059	1.047	1.1	1.375	1.933	28.8	8.072	8.159	1.1	16.12	19.11	15.6
Trefoil	0.0009	0.0067	86.6	0.0241	0.3577	93.3	0.1569	0.2299	31.8	0.1027	0.4146	75.2
δTrefoil	0.0290	0.0446	35.0	0.0631	0.6623	90.5	0.4145	0.5294	21.7	0.2776	0.6953	60.1

	Offloader C (DOF 3)			Offloader C (DOF 4)			Offloader C (DOF5)			Offloader C (DOF 6)		
	EKC	SAO	%	EKC	SAO	%	EKC	SAO	%	EKC	SAO	%
Decent	11.29	10.14	11.4	2.410	0.2680	799	1.605	1.438	11.6	2.518	2.282	10.4
Tilt	3.985	3.582	11.3	0.6459	0.0805	702	0.5637	0.5041	11.8	0.5453	0.5228	4.3
Oval.	0.1485	0.3058	51.4	0.0598	0.0197	204	0.0697	0.0986	29.3	1.021	1.267	19.4
$\delta\delta_r$	8.850	8.820	0.3	2.118	0.2700	685	1.281	1.274	0.5	1.375	1.554	11.5
Trefoil	0.0030	0.0011	173	0.0161	0.0039	313	0.0009	0.0021	57.1	0.0210	0.0052	304
δTrefoil	0.1119	0.1399	20.0	0.1200	0.0048	2400	0.0290	0.0360	19.4	0.0547	0.0023	2278

P6 OPTIC

unit in μin

	Hard Point A (DOF 1)			Hard Point A (DOF 4)			Hard Point A (DOF5)			Hard Point A (DOF 6)		
	EKC	SAO	%	EKC	SAO	%	EKC	SAO	%	EKC	SAO	%
Decent	25.94	23.82	8.9	3.508	0.6142	471	0.7370	0.6529	12.9	2.243	2.034	10.3
Tilt	7.008	6.243	12.2	0.7379	0.1679	339	0.3040	0.2688	13.2	0.4806	0.4226	13.7
Oval.	5.559	6.212	10.5	0.0402	0.1638	75	0.0198	0.0308	35.7	0.4271	0.4773	10.5
δδ r	8.861	9.307	4.8	1.061	0.5333	99	0.3057	0.3088	1.0	0.6762	0.7026	6.3
Trefoil	0.0193	0.0251	23.1	0.0013	0.0002	550	0.0003	0.0002	50.0	0.0044	0.0058	23.7
δTrefoil	0.0875	0.1097	20.2	0.0243	0.0025	860	0.0066	0.0080	17.5	0.0200	0.0249	19.7

	Offloader B (DOF 1)			Offloader B (DOF 2)			Offloader B (DOF3)			Offloader B (DOF 4)		
	EKC	SAO	%	EKC	SAO	%	EKC	SAO	%	EKC	SAO	%
Decent	19.33	17.76	8.8	12.22	11.25	8.7	3.957	3.539	11.8	1.904	0.4184	355
Tilt	4.719	4.201	12.3	3.146	2.807	12.1	1.492	1.340	11.3	0.7870	0.6626	18.8
Oval.	4.149	4.636	10.5	2.604	2.018	10.6	0.0430	0.0105	309	0.0426	0.0555	23.2
δδ r	6.605	6.036	4.8	4.174	4.389	4.9	1.770	1.804	1.9	0.9696	1.011	4.1
Trefoil	0.0193	0.0253	23.7	0.0088	0.0116	24.1	0.0016	0.0015	6.7	0.0013	0.0140	90.7
δTrefoil	0.0875	0.1099	20.4	0.0416	0.0524	20.6	0.0127	0.0157	19.1	0.0243	0.1705	85.7

	Offloader B (DOF 5)			Offloader B (DOF 6)			Offloader C (DOF1)			Offloader C (DOF 2)		
	EKC	SAO	%	EKC	SAO	%	EKC	SAO	%	EKC	SAO	%
Decent	0.9488	0.8452	12.3	1.851	1.6826	10.0	7.737	7.037	9.9	17.30	15.93	8.6
Tilt	0.2853	0.2524	13.0	0.5499	0.4860	13.1	2.333	2.079	12.2	4.326	3.855	12.2
Oval.	0.0176	0.0314	43.9	0.4271	0.4773	10.5	1.877	2.095	10.4	3.683	4.118	10.6
δδ r	0.4128	0.4180	1.2	0.6762	0.7025	3.7	2.958	3.100	4.6	5.903	6.208	4.9
Trefoil	0.0003	0.0002	50.0	0.0040	0.0052	23.1	0.0193	0.0252	23.4	0.0125	0.0165	24.2
δTrefoil	0.0071	0.0079	10.1	0.0179	0.0223	19.7	0.0875	0.1099	20.4	0.0588	0.0740	20.5

	Offloader C (DOF 3)			Offloader C (DOF 4)			Offloader C (DOF5)			Offloader C (DOF 6)		
	EKC	SAO	%	EKC	SAO	%	EKC	SAO	%	EKC	SAO	%
Decent	5.516	4.931	11.9	1.781	0.1560	1041	1.054	0.9385	12.3	1.944	1.774	9.6
Tilt	2.108	1.893	11.3	0.4245	0.0318	1235	0.3932	0.3498	12.4	0.4396	0.3870	13.6
Oval.	0.0608	0.0149	308	0.0449	0.0005	8880	0.0151	0.0320	52.8	0.4271	0.4773	10.5
δδ r	2.504	2.551	1.9	0.8691	0.0969	797	0.4974	0.5041	1.3	0.6762	0.7025	3.7
Trefoil	0.0023	0.0021	9.5	0.0013	0.0002	550	0.0003	0.0002	50.0	0.0034	0.0045	24.4
δTrefoil	0.0180	0.0222	18.9	0.0243	0.0025	872	0.0071	0.0079	10.1	0.0155	0.0192	19.3

H1 OPTIC

unit in μin

	Hard Point A (DOF 1)			Hard Point A (DOF 4)			Hard Point A (DOF5)			Hard Point A (DOF 6)		
	EKC	SAO	%	EKC	SAO	%	EKC	SAO	%	EKC	SAO	%
Decent	26.36	22.72	16.0	2.268	0.3686	515	0.5545	0.4478	23.8	1.423	1.107	28.5
Tilt	4.611	3.859	19.5	0.5263	0.1240	324	0.1624	0.1279	27.0	0.2172	0.1826	18.9
Oval.	12.67	18.49	31.5	0.0946	0.0435	118	0.0012	0.0690	98.3	0.5648	0.9063	37.7
δδ r	16.74	18.17	7.9	1.822	0.5149	254	0.5926	0.5538	7.0	0.8019	0.8666	7.5
Trefoil	0.0008	0.0845	99.1	0.0205	0.0103	99.0	0.0065	0.0054	20.4	0.0010	0.1709	99.4
δTrefoil	0.6082	0.5149	18.1	0.1508	0.0266	467	0.0457	0.0361	26.6	0.0872	0.2692	67.6

	Offloader B (DOF 1)			Offloader B (DOF 2)			Offloader B (DOF3)			Offloader B (DOF 4)		
	EKC	SAO	%	EKC	SAO	%	EKC	SAO	%	EKC	SAO	%
Decent	20.10	17.26	16.4	12.58	10.85	16.0	4.662	3.786	23.1	1.432	0.2605	450
Tilt	3.392	2.914	16.4	2.182	1.849	18.0	1.697	1.308	29.8	0.4947	0.0902	448
Oval.	9.457	14.05	32.7	5.934	8.764	32.3	1.008	0.5849	72.3	0.0705	0.0425	65.9
δδ r	12.47	13.76	9.4	7.914	8.695	9.0	5.493	5.394	1.8	1.659	0.3732	345
Trefoil	0.0008	1.098	99.9	0.0020	0.4296	99.5	0.0270	0.0477	43.4	0.0205	0.0035	486
δTrefoil	0.6082	1.774	65.7	0.2928	0.7097	58.7	0.1294	0.1907	32.1	0.1508	0.0116	120

	Offloader B (DOF 5)			Offloader B (DOF 6)			Offloader C (DOF1)			Offloader C (DOF 2)		
	EKC	SAO	%	EKC	SAO	%	EKC	SAO	%	EKC	SAO	%
Decent	0.7655	0.6225	23.0	1.147	0.9373	22.4	7.971	6.949	14.7	17.91	15.43	16.1
Tilt	0.2259	0.1831	23.4	0.2271	0.1589	42.9	1.556	1.188	31.0	3.063	2.622	16.8
Oval.	0.0455	0.0741	38.6	0.5648	0.7791	27.5	4.279	5.760	25.7	8.392	12.47	32.7
δδ r	0.7841	0.7791	0.6	0.8019	0.7463	7.5	5.547	5.572	0.5	11.19	12.35	9.4
Trefoil	0.0065	0.0391	83.4	0.0009	0.0112	92.0	0.0008	0.0825	99.0	0.0028	0.7764	99.6
δTrefoil	0.0457	0.0915	50.1	0.0786	0.0608	29.3	0.6082	0.5223	16.4	0.4141	1.259	67.1

	Offloader C (DOF 3)			Offloader C (DOF 4)			Offloader C (DOF5)			Offloader C (DOF 6)		
	EKC	SAO	%	EKC	SAO	%	EKC	SAO	%	EKC	SAO	%
Decent	6.569	5.339	23.0	1.430	0.1105	1194	0.8416	0.6919	21.6	1.260	1.012	24.5
Tilt	2.404	1.848	30.1	0.3990	0.0373	970	0.2816	0.2159	30.4	0.2135	0.1673	27.6
Oval.	1.425	0.8394	69.7	0.0314	0.0174	80.0	0.0644	0.0232	178	0.5648	0.8389	32.7
δδ r	7.769	7.617	2.0	1.477	0.1587	831	0.9373	0.9056	3.5	0.8019	0.7954	0.8
Trefoil	0.0382	0.0630	39.4	0.0205	0.0038	439	0.0065	0.0068	4.4	0.0008	0.0988	99.2
δTrefoil	0.1830	0.2102	12.9	0.1508	0.0176	757	0.0457	0.0411	11.2	0.0689	0.1611	57.2

H3 OPTIC

unit in μin

	Hard Point A (DOF 1)			Hard Point A (DOF 4)			Hard Point A (DOF5)			Hard Point A (DOF 6)		
	EKC	SAO	%	EKC	SAO	%	EKC	SAO	%	EKC	SAO	%
Decent	34.61	31.79	8.9	3.595	0.5714	529	0.8118	0.7069	14.8	2.302	1.990	15.7
Tilt	6.841	5.918	15.6	0.8056	0.1982	306	0.2432	0.2064	17.8	0.3903	0.3129	24.7
Oval.	13.11	14.54	9.8	0.1258	0.1023	23.0	0.0058	0.0136	57.4	0.7261	0.8063	9.9
δδ r	22.49	18.68	20.4	2.610	0.5688	359	0.8095	0.6637	22.0	1.318	1.016	29.7
Trefoil	0.0094	0.0321	70.7	0.0216	0.0020	980	0.0063	0.0044	43.2	0.0023	0.0055	58.2
δTrefoil	0.6116	0.4665	31.1	0.1659	0.0090	1743	0.0470	0.0352	33.5	0.1073	0.0763	40.6

	Offloader B (DOF 1)			Offloader B (DOF 2)			Offloader B (DOF3)			Offloader B (DOF 4)		
	EKC	SAO	%	EKC	SAO	%	EKC	SAO	%	EKC	SAO	%
Decent	26.31	24.20	8.7	16.48	15.16	8.7	5.488	4.790	14.6	2.196	0.4070	440
Tilt	4.984	4.315	15.5	3.212	2.786	15.3	1.979	1.746	13.3	0.7662	0.1476	419
Oval.	9.786	10.85	9.8	6.141	6.815	9.9	0.9627	0.8760	9.9	0.0959	0.0762	25.9
δδ r	16.76	13.92	20.4	10.61	8.826	20.2	5.898	4.872	21.0	2.392	0.4237	464
Trefoil	0.0094	0.0322	70.8	0.0055	0.0140	60.7	0.0200	0.0176	13.6	0.0216	0.0020	980
δTrefoil	0.6116	0.4669	31.0	0.2918	0.2239	30.3	0.1016	0.0775	31.1	0.1660	0.0090	1744

	Offloader B (DOF 5)			Offloader B (DOF 6)			Offloader C (DOF1)			Offloader C (DOF 2)		
	EKC	SAO	%	EKC	SAO	%	EKC	SAO	%	EKC	SAO	%
Decent	1.113	0.9790	13.7	1.861	1.626	14.5	10.50	9.584	9.5	23.45	21.58	8.6
Tilt	0.3265	0.2848	14.6	0.4102	0.3296	24.5	2.307	1.994	15.7	4.500	3.902	15.3
Oval.	0.0573	0.0399	43.6	0.7261	0.8063	9.9	4.427	4.900	9.6	8.685	9.638	9.9
δδ r	1.065	0.8746	21.7	1.318	1.016	29.7	7.483	6.199	20.7	15.01	12.48	20.2
Trefoil	0.0063	0.0044	43.2	0.0021	0.0049	57.1	0.0094	0.0324	71.0	0.0078	0.0199	60.8
δTrefoil	0.0470	0.0352	33.5	0.0966	0.0681	41.9	0.6116	0.4666	31.1	0.4127	0.3162	30.5

	Offloader C (DOF 3)			Offloader C (DOF 4)			Offloader C (DOF5)			Offloader C (DOF 6)		
	EKC	SAO	%	EKC	SAO	%	EKC	SAO	%	EKC	SAO	%
Decent	7.723	6.739	14.6	2.194	0.1723	1173	1.222	1.069	14.3	2.028	1.778	14.0
Tilt	2.802	2.473	13.3	0.6022	0.0520	1058	0.4108	0.3594	14.3	0.3797	0.3052	24.4
Oval.	1.362	1.239	9.9	0.0507	0.0340	49.1	0.0809	0.0547	47.9	0.7261	0.8062	9.9
δδ r	8.341	6.891	21.0	2.150	0.1887	1040	1.270	1.044	21.6	1.318	1.016	29.7
Trefoil	0.0283	0.0249	13.7	0.0216	0.0020	980	0.0063	0.0044	43.2	0.0019	0.0044	56.8
δTrefoil	0.1437	0.1100	30.6	0.1660	0.0090	1744	0.0470	0.0352	33.5	0.0846	0.0588	43.9

H4 OPTIC

unit in μin

	Hard Point A (DOF 1)			Hard Point A (DOF 4)			Hard Point A (DOF5)			Hard Point A (DOF 6)		
	EKC	SAO	%	EKC	SAO	%	EKC	SAO	%	EKC	SAO	%
Decent	35.54	32.81	8.3	4.082	0.6365	541	0.8828	0.7704	14.6	2.666	2.333	14.3
Tilt	7.432	6.521	14.0	0.8873	0.2186	306	0.2696	0.2243	20.2	0.4719	0.3879	21.7
Oval.	11.39	16.18	29.6	0.1324	0.1275	3.8	0.0091	0.0117	22.2	0.7136	1.015	29.7
δδ r	21.21	21.96	3.4	2.555	0.6780	277	0.7783	0.7993	2.6	1.395	1.353	3.1
Trefoil	0.0043	0.1960	97.8	0.0161	0.0066	144	0.0045	0.0111	59.5	0.0003	0.0370	99.2
δTrefoil	0.4210	0.5239	19.6	0.1200	0.0131	816	0.0332	0.0479	30.7	0.0829	0.0967	14.3

	Offloader B (DOF 1)			Offloader B (DOF 2)			Offloader B (DOF3)			Offloader B (DOF 4)		
	EKC	SAO	%	EKC	SAO	%	EKC	SAO	%	EKC	SAO	%
Decent	26.97	24.94	8.1	16.90	15.65	8.0	5.254	4.669	12.5	2.412	0.4458	441
Tilt	5.371	4.719	13.8	3.473	3.059	13.5	1.906	1.721	10.7	0.8543	0.1626	444
Oval.	8.499	12.08	29.6	5.333	7.591	29.7	0.8219	0.9628	14.6	0.1027	0.0950	8.1
δδ r	15.81	16.36	3.4	10.00	10.38	3.6	4.949	5.125	3.4	2.347	0.5053	364
Trefoil	0.0043	0.0245	82.4	0.0012	0.0889	98.7	0.0137	0.0500	72.6	0.0161	0.0066	144
δTrefoil	0.4210	0.5240	19.7	0.2004	0.2526	20.7	0.0621	0.0992	37.4	0.1200	0.0131	816

	Offloader B (DOF 5)			Offloader B (DOF 6)			Offloader C (DOF1)			Offloader C (DOF 2)		
	EKC	SAO	%	EKC	SAO	%	EKC	SAO	%	EKC	SAO	%
Decent	1.205	1.075	12.2	2.152	1.897	13.4	10.76	9.851	9.2	24.04	22.26	8.0
Tilt	0.3511	0.3104	13.1	0.5001	0.4121	21.4	2.504	2.196	14.0	4.855	4.274	13.6
Oval.	0.0581	0.0525	10.7	0.7136	1.015	29.7	3.846	5.450	29.4	7.542	10.73	29.7
δδ r	1.021	1.050	2.8	1.395	1.353	3.1	7.064	7.288	3.1	14.14	14.67	3.6
Trefoil	0.0045	0.0111	59.5	0.0002	0.0333	99.4	0.0043	0.1959	97.8	0.0018	0.1257	98.6
δTrefoil	0.0332	0.0479	30.7	0.0746	0.0863	13.6	0.4210	0.5240	19.7	0.2835	0.3574	20.7

	Offloader C (DOF 3)			Offloader C (DOF 4)			Offloader C (DOF5)			Offloader C (DOF 6)		
	EKC	SAO	%	EKC	SAO	%	EKC	SAO	%	EKC	SAO	%
Decent	7.386	6.561	12.6	2.410	0.1835	1214	1.319	1.170	12.7	2.336	2.068	12.9
Tilt	2.697	2.433	10.8	0.6459	0.0508	1171	0.4472	0.3980	12.4	0.4553	0.3756	21.2
Oval.	1.162	1.362	14.6	0.0598	0.0425	40.7	0.0817	0.0733	11.5	0.7136	1.015	29.7
δδ r	6.999	7.247	3.4	2.118	0.2255	83.9	1.215	1.252	2.9	1.395	1.353	3.1
Trefoil	0.0194	0.0708	72.6	0.0161	0.0066	144	0.0045	0.0111	59.5	0.0002	0.0287	99.3
δTrefoil	0.0879	0.1402	37.3	0.1200	0.0131	816	0.0332	0.0479	30.7	0.0652	0.0745	12.5

H6 OPTIC

unit in μin

	Hard Point A (DOF 1)			Hard Point A (DOF 4)			Hard Point A (DOF5)			Hard Point A (DOF 6)		
	EKC	SAO	%	EKC	SAO	%	EKC	SAO	%	EKC	SAO	%
Decent	20.78	18.94	9.7	3.167	0.4223	1360	0.5950	0.5110	16.4	2.080	1.814	14.7
Tilt	4.867	4.272	13.9	0.6108	0.1551	294	0.1965	0.1670	17.7	0.3893	0.3278	18.8
Oval.	2.526	3.253	22.3	0.1020	0.0331	208	0.0192	0.0002	9500	0.2106	0.2727	22.8
δδ r	7.761	5.748	35.0	1.061	0.1788	493	0.3096	0.2162	43.2	0.6705	0.4754	41.0
Trefoil	0.0008	0.0050	84.0	0.0038	0.0003	1167	0.0010	0.0007	42.9	0.0003	0.0011	63.6
δTrefoil	0.0886	0.0603	46.9	0.0270	0.0011	2355	0.0071	0.0045	57.8	0.0228	0.0147	55.1

	Offloader B (DOF 1)			Offloader B (DOF 2)			Offloader B (DOF3)			Offloader B (DOF 4)		
	EKC	SAO	%	EKC	SAO	%	EKC	SAO	%	EKC	SAO	%
Decent	15.68	14.32	9.5	9.873	9.019	9.5	2.668	2.385	11.9	1.632	0.2922	459
Tilt	3.389	2.977	13.8	2.237	1.971	13.5	1.068	0.979	9.1	0.6397	0.1154	454
Oval.	1.886	2.426	22.3	1.181	1.526	22.6	0.2767	0.1867	48.2	0.0872	0.0246	254
δδ r	5.785	4.280	35.2	3.660	2.715	34.8	1.428	1.011	41.3	0.9798	0.1332	636
Trefoil	0.0008	0.0043	81.4	0.0005	0.0019	73.7	0.0022	0.0019	15.8	0.0038	0.0003	1167
δTrefoil	0.0886	0.0589	50.4	0.0423	0.0286	47.9	0.0091	0.0061	49.2	0.0270	0.0011	2355

	Offloader B (DOF 5)			Offloader B (DOF 6)			Offloader C (DOF1)			Offloader C (DOF 2)		
	EKC	SAO	%	EKC	SAO	%	EKC	SAO	%	EKC	SAO	%
Decent	0.8121	0.7106	14.3	1.648	1.459	13.0	6.140	5.592	9.8	14.02	12.81	9.4
Tilt	0.2302	0.2019	14.0	0.4355	0.3674	18.5	1.643	1.440	14.1	3.090	2.720	13.6
Oval.	0.0391	0.0159	14.6	0.2106	0.2727	22.8	0.8563	1.095	21.8	1.670	2.158	22.6
δδ r	0.4029	0.2820	42.9	0.6705	0.4754	41.0	2.586	1.906	36.2	5.175	3.894	34.8
Trefoil	0.0010	0.0007	42.9	0.0003	0.0010	70.0	0.0008	0.0043	81.4	0.0008	0.0026	69.2
δTrefoil	0.0071	0.0045	57.8	0.0205	0.0131	56.5	0.0886	0.0593	49.4	0.0598	0.0403	48.4

	Offloader C (DOF 3)			Offloader C (DOF 4)			Offloader C (DOF5)			Offloader C (DOF 6)		
	EKC	SAO	%	EKC	SAO	%	EKC	SAO	%	EKC	SAO	%
Decent	3.724	3.328	11.9	1.622	0.1004	1516	0.8721	0.7639	14.2	1.778	1.579	12.6
Tilt	1.494	1.365	9.5	0.3589	0.0137	2520	0.3177	0.2819	12.7	0.3617	0.3069	17.9
Oval.	0.3913	0.2640	48.2	0.0693	0.0110	530	0.0519	0.0225	130	0.2106	0.2727	22.8
δδ r	2.020	1.429	41.3	0.8919	0.0593	1404	0.4783	0.3353	42.6	0.6705	0.4754	41.0
Trefoil	0.0031	0.0026	19.2	0.0038	0.0003	1167	0.0010	0.0007	42.9	0.0003	0.0009	66.7
δTrefoil	0.0129	0.0087	48.3	0.0270	0.0011	2355	0.0071	0.0045	57.8	0.0179	0.0114	57.0

APPENDIX B

SAO MEMO: EKC MAS FORCE SENSITIVITY ANALYSIS COMPARISON

MEMORANDUM

To:	W. Podgorski
From:	J.P. Zhang
Date:	August 20, 1993
File:	/usr/people/jzhang/wp/jpz93_16
Subject:	EKC MAS force sensitivity analysis comparison - Continued
Reference:	EKC Monitoring -2300
Copies:	R. Brissenden, F. Cocuzzo, L. Cohen, K. Daigle, R. Dias, R. Goddard, E. Kellogg, M. Freeman, P. Hsieh, J. Hughes, P. McKinnon, E. McLaughlin, D. Schwartz, A. Szentgyorgyi, P. Slane, H. Tananbaum, L. VanSpeybroeck

SUMMARY

This memo is a follow up of EKC mirror assembly station (MAS) force sensitivity comparison documented on July 29,1993(/usr/people/jzhang/wp/jpz93_15). Finite Element Analysis (FEA) for both P1 and P6 mirrors is completed. Results in terms of Legendre-Fourier coefficients which represent decenter, tilt, ovalization, delta-delta R, trefoil, and delta trefoil are compared with those analyzed by Kodak.

To complete the full MAS force sensitivity study, independent FEA analysis at one hard point A in 4 degree of freedom (DOF) and two offloaders B and C in 6 DOF is sufficient since results at all other hard points a and offloaders b, c can be derived from them (ref. figure 1). In each independent analysis, a unit load (force or moment, depending on its DOF) is applied at the hard point A or offloader B or C. Our results show that for the p1 mirror, the Legendre-Fourier coefficients are within an average range of 12% except in DOF 4 (moment in radial direction) where an average error of 351%, 402% and 537% is found at hard point A, offloader B and C, respectively. The comparison of p6 mirror results in a similar pattern as of p1 mirror, though a 308% difference in ovalization exits for all unrestrained DOF 3. A further raytrace study on Legendre-Fourier coefficient sensitivity shows that errors in most coefficients are negligible since they are posted on very small numbers. However the disagreement on delta-delta R in DOF 4 could have a noticeable impact on MAS performance prediction, depending on the allowable force.

An effort of trying to figure out the cause of the difference in DOF 4 has been made by analysing different shell and solid element FEA models since a shell element FEA model is used by Kodak while a solid elements model by SAO. A consistent result is observed for solid elements models while result from shell elements model is mesh dependent due to the fact that a shell element can not sustain a moment perpendicular to its plane.

DISCUSSION

A 180 degree SDRC-IDEAS FEA model is used in the analysis at hard point A (DOF 1 and 5) and offloader C (DOF 1, 3, and 5) due to the symmetry of the geometry and loading in the problem, as shown in figure 2. Figure 3 shows a 360 degree FEA model used for the remaining DOFs at A, B, and C. Figures 4 and 5 show boundary conditions for half and whole model, respectively. In each independent analysis, a superposition analysis method is applied to simulate the mirror MAS force sensitivity (ref. /usr/people/jzhang/wp/jpz93_15). Figures 6 through 8 show coupled forces applied at mirror nodes to form a unit moment in DOF 4, 5, and 6, respectively. The comparison of Legendre-Fourier coefficients with Kodak for both p1 and p6 mirrors is listed in table 1. The results obtained at SAO are within a reasonable range with Kodak except in DOF 4 at hard point and both offloaders for both mirrors and a large difference in ovalization in DOF 3 at offloaders for p6 mirror only.

Finite element analysis on both solid element (used at SAO) and shell element (used at EKC) models (mirror only), has been conducted to trace the cause of a large disagreement in DOF 4 at all three points A, B, and C. Based on the fact that in FEA model SAO uses solid elements of a 2.5 degree segment circumferentially while Kodak uses shell elements of a 5.0 degree segment, two test models, a 5 degree segment solid model and a 7.5 degree segment shell model, were generated. FEA results are compared with original models, as shown in table 2. A consistent result is observed for solid element models, while a mesh dependent result is shown for shell element models. Since a shell element can not sustain a bending moment perpendicular to its plane, a continuing reduce the mesh size circumferentially will result a larger deformation or even singularity as the angle between a bending moment (in DOF 4) and the norm of the shell element plane tends to 90 degree.

In order to determine qualitatively the impact on MAS performance prediction due to the disagreement on MAS force sensitivity analysis between EKC and SAO, raytrace of 6 cases for each p1 and p6 mirror is studied. In each case, one out of six Legendre-Fourier coefficients(decenter, tilt, ovalization, delta-delta R, trefoil, and delta trefoil) is singled out by setting others to zero in raytrace analysis. Table 3 shows 90% EE and RMS diameter caused by each individual Legendre-Fourier coefficients. A value of 10 microinch is applied to each coefficient except tilt where a value of 0.1 arcsecond is used. Raytrace results listed in table 3 can be easily scaled to obtain 90% EE and RMS diameter for all DOFs at points A, B, and C. Table 4 lists 90% EE diameter for both p1 and p6 mirror in DOF 4 at hard point A. The difference in 90% EE diameter is listed in table 1 under colum "%" for errors between EKC and SAO larger than 20%. Results show that the disagreement on Legendre-Fourirer coefficients provides a negligible impact on 90% EE diameter except delta-delta R term where the difference in 90% EE diameter reaches 0.06 arcsecond(ref. DOF 4) for the 1 in-lb applied load.

FUTURE WORK

It is our intent to perform a Monte-Carlo analysis of the result, obtained to date as part of our on-going verification of EKC FEA work.

TABLE 1 P1 & P6 Optic – Residual errors due to unit MAS errors

HARD POINT A, DOF 1

	P1			P6		
	EKC	**SAO**	**%** (δ90% ee)	**EKC**	**SAO**	**%** (δ90% ee)
Decenter	32.8042	30.8272	6.4	25.9449	23.8222	8.9
Tilt	7.1111	6.2979	12.9	7.0079	6.2434	12.2
Oval	19.2537	21.1016	8.8	5.5594	6.2120	10.5
Δ–Δ R	18.7017	17.1513	9.0	8.8608	9.3070	4.8
Trefoil	0.2663	0.3348	20.5 (NEG*)	0.0193	0.0251	23.1 (NEG)
Δ–Trefoil	0.5474	0.5781	5.3	0.0875	0.1097	20.2 (0.001)
Avg. Error			10.5			13.3

Unit in μin

* NEG – negligible, δ(90% ee diameter) <<0.001

HARD POINT A, DOF 4

	P1			P6		
	EKC	**SAO**	**%** (δ90% ee)	**EKC**	**SAO**	**%** (δ90% ee)
Decenter	2.5254	0.5838	333 (0.001)	3.5075	0.6142	471 (0.002)
Tilt	0.6194	0.1621	282 (0.012)	0.7379	0.1679	339 (0.015)
Oval	0.1483	0.0308	381 (NEG)	0.0402	0.1638	75 (NEG)
Δ–Δ R	1.7701	0.5829	204 (0.061)	1.0607	0.5333	99 (0.027)
Trefoil	0.0099	0.0006	155 (NEG)	0.0013	0.0002	550 (NEG)
Δ–Trefoil	0.1101	0.0129	753 (0.005)	0.0243	0.0025	860 (0.001)
Avg. Error			351			399

Unit in μin

TABLE 1 – Cont'd

POINT A, DOF 5

	P1			P6		
	EKC	SAO	% (δ90% ee)	EKC	SAO	% (δ90% ee)
Decenter	0.6487	0.5729	13.2	0.7370	0.6529	12.9
Tilt	0.2344	0.2062	13.7	0.3040	0.2688	13.2
Oval	0.0567	0.0614	7.7	0.0198	0.0308	35.7 (NEG)
Δ–Δ R	0.5692	0.5167	10.2	0.3057	0.3088	1.0
Trefoil	0.0027	0.0034	20.6 (NEG)	0.0003	0.0002	50.0 (NEG)
Δ–Trefoil	0.0350	0.0363	3.6	0.0066	0.0080	17.5
Avg. Error			11.5			21.7

Unit in μin

HARD POINT A, DOF 6

	P1			P6		
	EKC	SAO	% (δ90% ee)	EKC	SAO	% (δ90% ee)
Decenter	1.4758	1.3899	6.2	2.2427	2.0339	10.3
Tilt	0.2632	0.2311	13.9	0.4806	0.4226	13.7
Oval	0.7848	0.8597	8.7	0.4271	0.4773	10.5
Δ–Δ R	0.7440	0.6790	9.6	0.6762	0.7026	6.3
Trefoil	0.0322	0.0405	20.5 (NEG)	0.0044	0.0058	23.7 (NEG)
Δ–Trefoil	0.0653	0.0687	4.9	0.0200	0.0249	19.7
Avg. Error			10.6			14.0

Unit in μin

TABLE 1 – Cont'd

OFFLOADER B, DOF 1

	P1			P6		
	EKC	SAO	% (δ90% ee)	EKC	SAO	% (δ90% ee)
Decenter	24.7149	23.2373	6.4	19.3286	17.7632	8.8
Tilt	4.9710	4.3870	13.3	4.7193	4.2011	12.3
Oval	14.3674	15.7420	8.7	4.1490	4.6356	10.5
Δ–Δ R	13.9352	12.7747	9.1	6.6054	6.0363	4.8
Trefoil	0.2663	0.3352	20.6 (NEG)	0.0193	0.0253	23.7 (NEG)
Δ–Trefoil	0.5475	0.5787	5.4	0.0875	0.1099	20.4 (0.001)
Avg. Error			10.6			13.4

Unit in μin

OFFLOADER B, DOF 2

	P1			P6		
	EKC	SAO	% (δ90% ee)	EKC	SAO	% (δ90% ee)
Decenter	15.5296	14.2562	8.9	12.2196	11.2459	8.7
Tilt	3.2576	3.0772	5.9	3.1460	2.8066	12.1
Oval	9.0243	10.7129	15.8	2.6040	2.0177	10.6
Δ–Δ R	8.8295	8.9921	1.8	4.1741	4.3894	4.9
Trefoil	0.1235	0.2622	52.9 (NEG)	0.0088	0.0116	24.1 (NEG)
Δ–Trefoil	0.2613	0.3418	23.6 (0.004)	0.0416	0.0524	20.6 (NEG)
Avg. Error			18.2			13.5

Unit in μin

TABLE 1 – Cont'd

OFFLOADER B, DOF 3

	P1			P6		
	EKC	SAO	% (δ90% ee)	EKC	SAO	% (δ90% ee)
Decenter	7.3036	6.4632	13.0	3.9572	3.5387	11.8
Tilt	2.4743	2.1844	13.3	1.4916	1.3403	11.3
Oval	0.2992	0.3246	7.8	0.0430	0.0105	309 (NEG)
Δ–Δ R	6.6942	6.1121	9.5	1.7704	1.8042	1.9
Trefoil	0.0053	0.0066	19.7	0.0016	0.0015	6.7
Δ–Trefoil	0.1427	0.1499	4.8	0.0127	0.0157	19.1
Avg. Error			11.4			60.0

Unit in μin

OFFLOADER B, DOF 4

	P1			P6		
	EKC	SAO	% (δ90% ee)	EKC	SAO	% (δ90% ee)
Decenter	1.6218	0.4034	302 (0.001)	1.9043	0.4184	355 (0.001)
Tilt	0.5940	0.1390	327 (0.012)	0.7870	0.6626	18.8
Oval	0.1399	0.0209	569 (NEG)	0.0426	0.0555	23.2 (NEG)
Δ–Δ R	1.5893	0.3926	305 (0.061)	0.9696	1.0110	4.1 (0.002)
Trefoil	0.0099	0.0006	155 (NEG)	0.0013	0.0140	90.7 (NEG)
Δ–Trefoil	0.1101	0.0129	753 (0.005)	0.0243	0.1705	85.7 (0.008)
Avg. Error			402			96.3

Unit in μin

TABLE 1 – Cont'd

OFFLOADER B, DOF 5

	P1			P6		
	EKC	SAO	% (δ90% ee)	EKC	SAO	% (δ90% ee)
Decenter	0.8937	0.7917	12.9	0.9488	0.8452	12.3
Tilt	0.2747	0.2401	14.4	0.2853	0.2524	13.0
Oval	0.0659	0.0713	7.6	0.0176	0.0314	43.9 (NEG)
Δ–Δ R	0.7857	0.7145	10.0	0.4128	0.4180	1.2
Trefoil	0.0027	0.0034	20.6 (NEG)	0.0003	0.0002	50.0 (NEG)
Δ–Trefoil	0.0350	0.0363	3.6	0.0071	0.0079	10.1
Avg. Error			11.5			21.8

Unit in μin

OFFLOADER B, DOF 6

	P1			P6		
	EKC	SAO	% (δ90% ee)	EKC	SAO	% (δ90% ee)
Decenter	1.2393	1.1588	6.9	1.8507	1.6826	10.0
Tilt	0.2894	0.2558	13.1	0.5499	0.4860	13.1
Oval	0.7848	0.8597	8.7	0.4271	0.4773	10.5
Δ–Δ R	0.7440	0.6790	9.6	0.6762	0.7025	3.7
Trefoil	0.0288	0.0363	20.7 (NEG)	0.0040	0.0052	23.1 (NEG)
Δ–Trefoil	0.0583	0.0612	4.8	0.0179	0.0223	19.7
Avg. Error			10.6			13.4

Unit in μin

TABLE 1 – Cont'd

OFFLOADER C, DOF 1

	P1			P6		
	EKC	SAO	% (δ90% ee)	EKC	SAO	% (δ90% ee)
Decenter	9.9919	9.2992	7.4	7.7369	7.0374	9.9
Tilt	2.3767	2.0995	13.2	2.3326	2.0786	12.2
Oval	6.4914	7.0964	8.5	1.8767	2.0946	10.4
Δ–Δ R	6.2148	5.6775	9.5	2.9577	3.0996	4.6
Trefoil	0.2663	0.3346	20.4 (NEG)	0.0193	0.0252	23.4 (NEG)
Δ–Trefoil	0.5475	0.5780	5.3	0.0875	0.1099	20.4 (0.001)
Avg. Error			10.7			13.5

Unit in μin

OFFLOADER C, DOF 2

	P1			P6		
	EKC	SAO	% (δ90% ee)	EKC	SAO	% (δ90% ee)
Decenter	22.0605	20.7837	6.1	17.3037	15.9298	8.6
Tilt	4.5279	4.0077	13.0	4.3260	3.8550	12.2
Oval	12.7623	14.0049	8.9	3.6827	4.1176	10.6
Δ–Δ R	12.4869	11.4732	8.8	5.9030	6.2076	4.9
Trefoil	0.1746	0.2201	20.7 (NEG)	0.0125	0.0165	24.2 (NEG)
Δ–Trefoil	0.3695	0.3921	5.8	0.0588	0.0740	20.5 (0.001)
Avg. Error			10.6			13.5

Unit in μin

TABLE 1 – Cont'd

OFFLOADER C, DOF 3

	P1			P6		
	EKC	SAO	% (δ90% ee)	EKC	SAO	% (δ90% ee)
Decenter	10.2305	9.0463	13.1	5.5162	4.9306	11.9
Tilt	3.5152	3.1036	13.3	2.1079	1.8934	11.3
Oval	0.4231	0.4591	7.8	0.0608	0.0149	308 (NEG)
Δ–Δ R	9.4671	8.6438	9.5	2.5038	2.5514	1.9
Trefoil	0.0075	0.0094	20.2 (NEG)	0.0023	0.0021	9.5
Δ–Trefoil	0.2018	0.2121	4.9	0.0180	0.0222	18.9
Avg. Error			11.5			60.3

Unit in μin

OFFLOADER C, DOF 4

	P1			P6		
	EKC	SAO	% (δ90% ee)	EKC	SAO	% (δ90% ee)
Decenter	1.5288	0.1797	751 (0.001)	1.7811	0.1560	1041 (0.001)
Tilt	0.4405	0.0524	741 (0.010)	0.4245	0.0318	1235 (0.011)
Oval	0.1311	0.0093	131 (NEG)	0.0449	0.0005	8880 (NEG)
Δ–Δ R	1.3850	0.1752	691 (0.062)	0.8691	0.0969	797 (0.040)
Trefoil	0.0099	0.0006	155 (NEG)	0.0013	0.0002	550 (NEG)
Δ–Trefoil	0.1101	0.0129	753 (0.005)	0.0243	0.0025	872 (0.001)
Avg. Error			537			2229

Unit in μin

TABLE 1 – Cont'd

OFFLOADER C, DOF 5

	P1			P6		
	EKC	SAO	% (δ90% ee)	EKC	SAO	% (δ90% ee)
Decenter	1.0202	0.8996	13.4	1.0543	0.9385	12.3
Tilt	0.3510	0.3081	13.9	0.3932	0.3498	12.4
Oval	0.0739	0.0801	7.7	0.0151	0.0320	52.8 (NEG)
Δ–Δ R	0.9543	0.8683	9.9	0.4974	0.5041	1.3
Trefoil	0.0027	0.0034	21.3 (NEG)	0.0003	0.0002	50.0 (NEG)
Δ–Trefoil	0.0350	0.0363	3.6	0.0071	0.0079	10.1
Avg. Error			11.7			23.2

Unit in μin

OFFLOADER C, DOF 6

	P1			P6		
	EKC	SAO	% (δ90% ee)	EKC	SAO	% (δ90% ee)
Decenter	1.3261	1.2444	6.6	1.9440	1.7742	9.6
Tilt	0.2508	0.2196	14.2	0.4396	0.3870	13.6
Oval	0.7848	0.8598	8.7	0.4271	0.4773	10.5
Δ–Δ R	0.7440	0.6792	9.5	0.6762	0.7025	3.7
Trefoil	0.0251	0.0316	20.6 (NEG)	0.0034	0.0045	24.4 (NEG)
Δ–Trefoil	0.0503	0.0528	4.7	0.0155	0.0192	19.3
Avg. Error			10.7			13.5

Unit in μin

TABLE 2

Shell and Solid Model Comparison – Optic only – Hard point supported

OFFLOADER B, DOF 4

	Solid Model (2.5 degree)	Solid Model (5.0 degree)	Shell Model (5.0 degree)	Shell Model (7.5 degree)
Decenter	0.4021	0.4012	0.9615	0.6721
Tilt	0.1521	0.1514	0.3888	0.2644
Ovalization	0.0150	0.0149	0.0991	0.0675
Δ–Δ R	0.5054	0.5048	1.3087	0.8977
Trefoil	0.0031	0.0031	0.0509	0.0329
Δ Trefoil	0.0570	0.0567	0.3377	0.2042

TABLE 3 Legendre–Fourier Coefficients Sensitivity

		P1		P6	
	Units	90% ee diam. (arcsec)	RMS diam. (arcsec)	90% ee diam. (arcsec)	RMS diam. (arcsec)
Decenter	10.0 μin	5.4957E–3	5.1203E–3	5.4948E–3	5.1223E–3
Tilt	0.1 arcsec	2.1621E–1	2.0146E–1	2.1715E–1	2.0230E–1
Ovalization	10.0 μin	1.0470E–2	8.0910E–3	1.0492E–2	8.1197E–3
Δ–Δ R	10.0 μin	5.1293E–1	3.5717E–1	5.1362E–1	3.5495E–1
Trefoil	10.0 μin	1.5693E–2	1.1479E–2	1.5746E–2	1.1569E–2
Δ Trefoil	10.0 μin	5.1290E–1	3.5542E–1	5.1413E–1	3.5480E–1

TABLE 4 P1 & P6 Optic, HP A, DOF4 – 90% EE diameter due to L–F coeff

	P1		P6	
	EKC 90% ee diam. (arcsec)	SAO 90 % ee diam. (arcsec)	EKC 90% ee diam. (arcsec)	SAO 90% ee diam. (arcsec)
Decenter	1.3879E–3	3.2084E–4	1.9273E–3	3.3749E–4
Tilt	1.6742E–2	4.3814E–3	1.9935E–2	4.5361E–3
Ovalization	1.5527E–4	3.2248E–5	4.2178E–5	1.7186E–4
Δ–Δ R	9.0793E–2	2.990E–2	5.4480E–2	2.7391E–2
Trefoil	1.5536E–5	9.4158E–7	2.0470E–6	3.1492E–7
Δ Trefoil	5.6470E–3	6.6164E–4	1.2493E–3	1.2493E–3

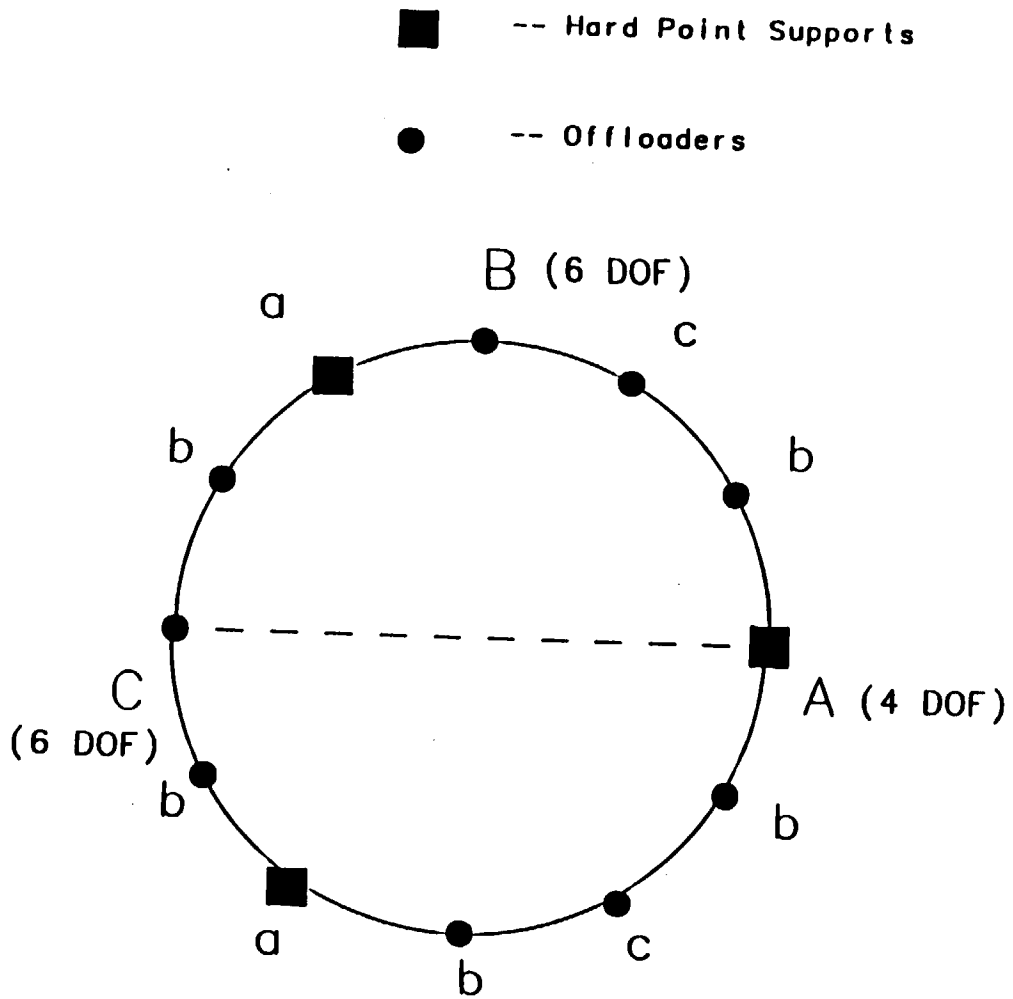
-- Hard Point Supports
-- Offloaders
B (6 DOF)
a
c
b
b
C
(6 DOF)
A (4 DOF)
b
b
a
b
c

Figure 1

Fig. 2

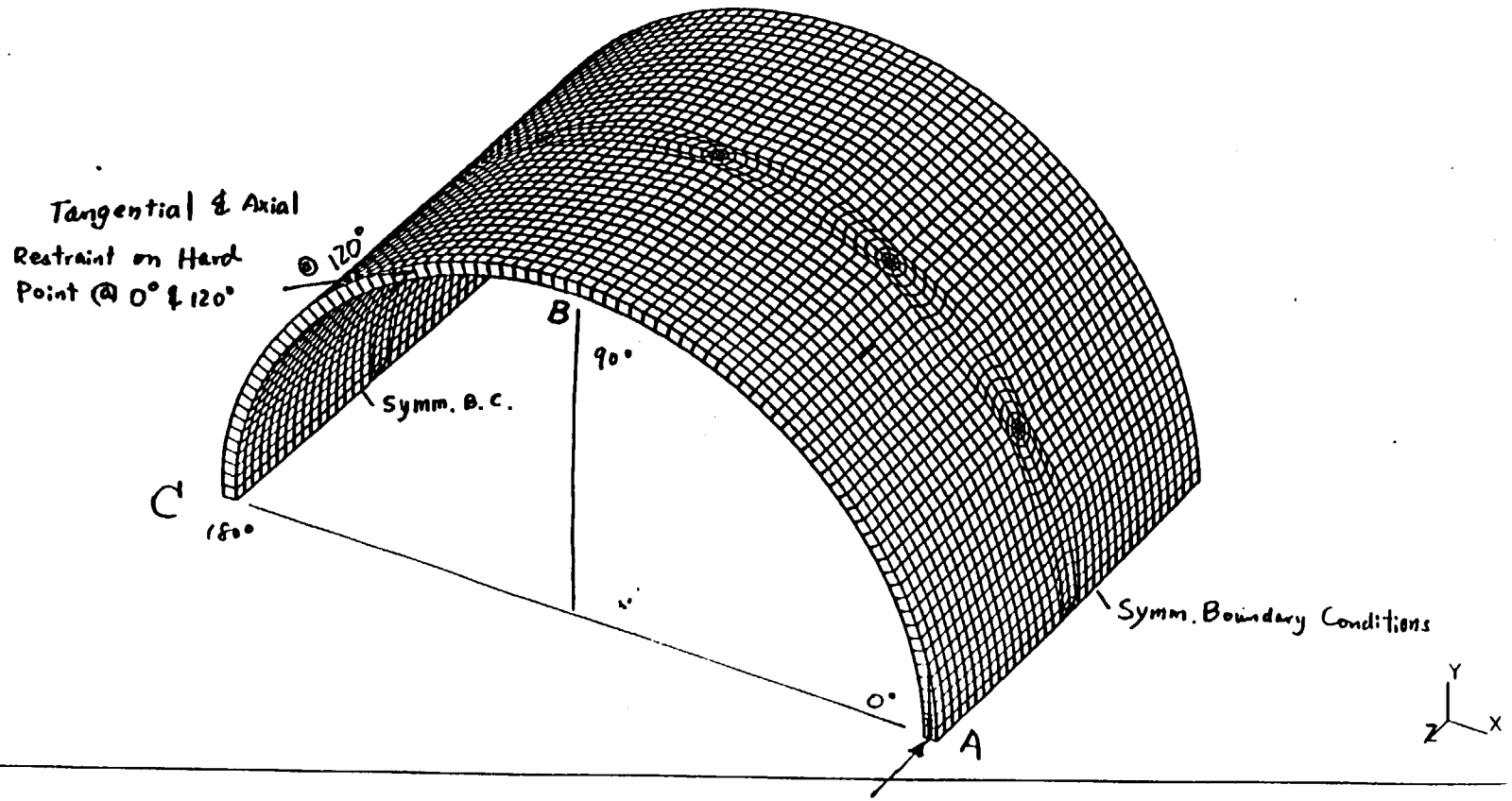
Tangential & Axial
Restraint on Hard
Point @ 0° & 120°
@ 120°
B
90°
Symm. B.C.
C
180°
0°
A
Symm. Boundary Conditions
Y
Z
X

Fig 3

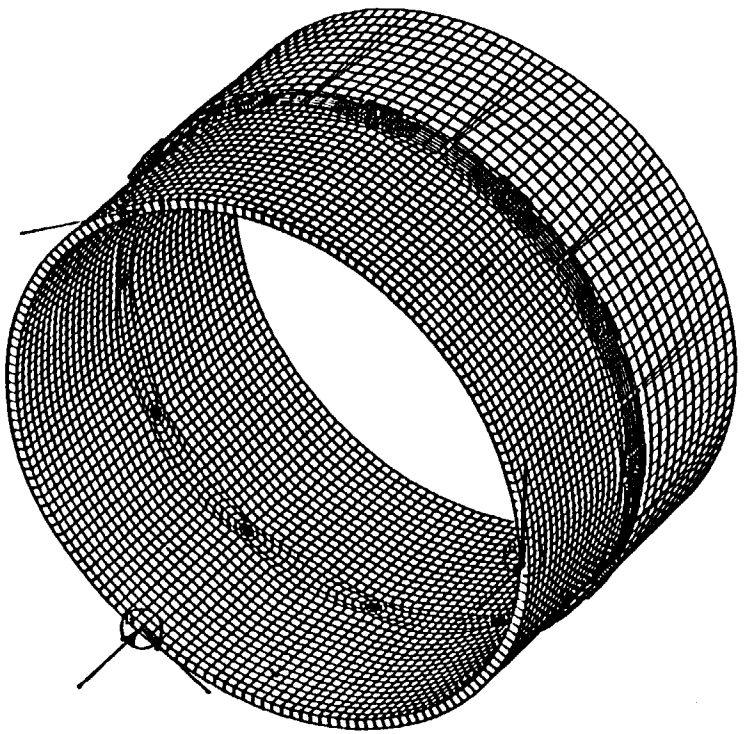

Tangential & Axial Restraint on
Hard Point @ 0°, 120° & 240°

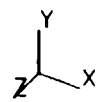

Fig. 4

Hard Point A, DOF 4

$M_1 = 2F_1 \times d_1 = 0.5$ in-lb

$M_2 = 2F_2 \times d_2 = 0.5$ in-lb

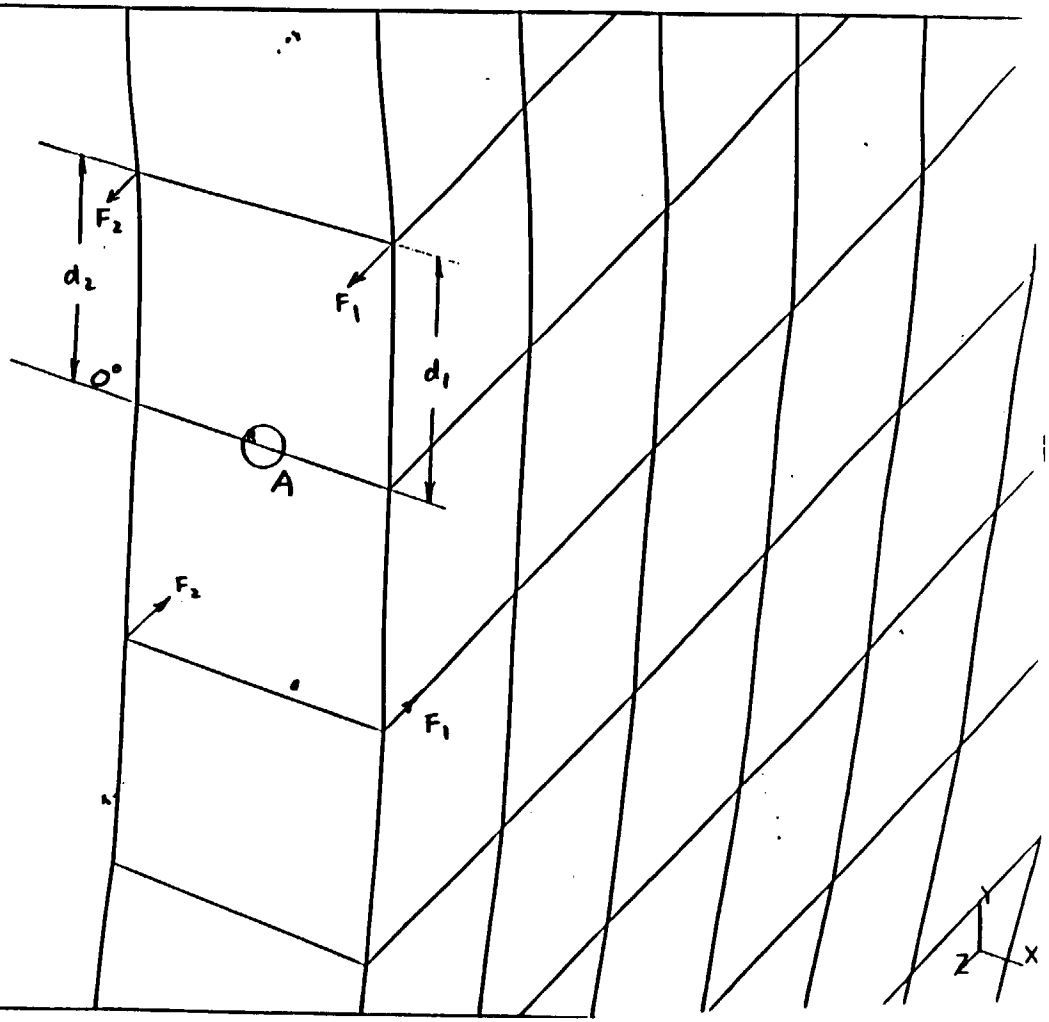

Fig 5

Hard point A, DOF 5

$M = F \times D = 1.0$ in-lb

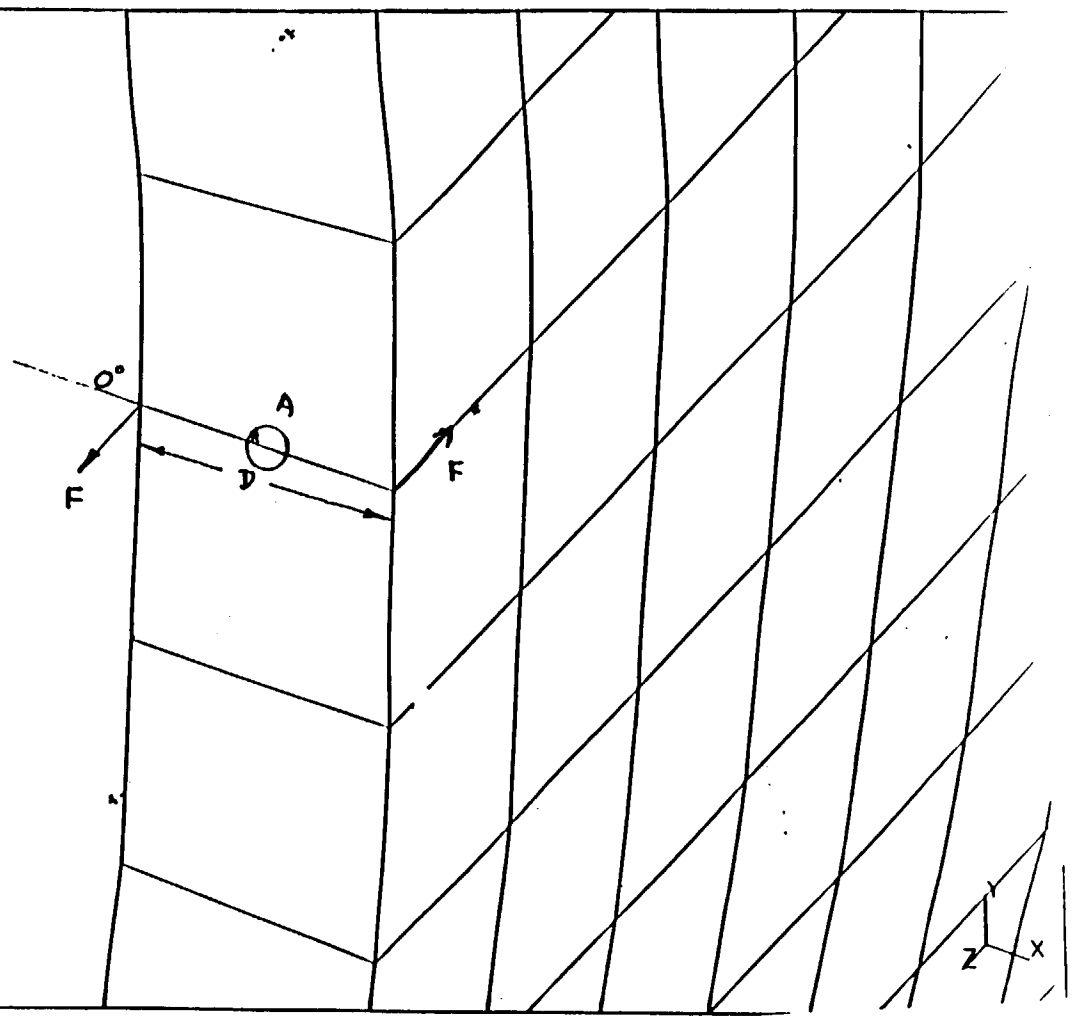

Fig 6

Hard Point A, DOF 6

$M = F * D = 1.0$ in-lb